A Study of Synovial Fluid through a Knee Joint



By

Javeria Javed

Registration No: 923-FOS/MSMA/F23

A Study of Synovial Fluid through a Knee Joint



By

Javeria Javed

Registration No: 923-FOS/MSMA/F23

Supervised by

Dr. Khadija Maqbool

A Study of Synovial Fluid through a Knee Joint By

Javeria Javed

Registration No: 923-FOS/MSMA/F23

A Thesis
Submitted in the Partial Fulfillment of the
Requirement for the Degree of
MASTER OF SCIENCE
In
MATHEMATICS

Supervised by

Dr. Khadija Maqbool

Certificate

A Study of Synovial Fluid through a Knee Joint

Javeria Javed

A DISSERTATION SUBMITTED IN THE PARTIAL FULFILLMENT
OF THE

REQUIREMENTS FORTHE DEGREE OF MASTER OF SCIENCE
IN MATHEMATICS

We accept this thesis as conforming to the required standard

1	2
Prof. Dr. Sadia Hina	Dr. Rabia Malik
(External Examiner)	(Internal Examiner)
3	4
Dr. Khadija Maqbool	Prof. Dr. Nasir Ali
(Supervisor)	(Chairman)

Thesis Certificate

The thesis entitled "A Study of Synovial Fluid through a Knee Joint" submitted by Javeria Javed, 923-FOS/MSMA/F23 in partial fulfillment of MS Degree in Mathematics has been completed under my guidance and supervision. I am satisfied with the quality of her research work and allow her to submit this thesis for further process to graduate with Master of Science degree from the Department of Mathematics & Statistics, as per IIUI rules and regulations.

D /		
Date		
2		

Dr. Khadija Maqbool
Assistant Professor
Department of Mathematics &
Statistics
International Islamic University,
Islamabad.

DECLARATION

I hereby declare that this thesis, neither as a whole nor a part of it, has been copied out from any source. It is further declared that I have prepared this dissertation entirely based on my efforts under the supervision of my supervisor **Dr. Khadija Maqbool**. No portion of the work, presented in this dissertation, has been submitted in the support of any application for any degree or qualification of this or any other learning institute.

Javeria Javed MS
(Mathematics)
Reg. No. 923-FOS/MSMA/F23
Department of Mathematics and Statistics
Faculty of Sciences,
International Islamic University Islamabad, Pakistan.

Dedication

To My Loving Family

Acknowledgments

All recommendations to Almighty Allah, who has disclosed upon me endurance and resoluteness for the accomplishment of this assignment. I offer my humblest and sincerest words of thanks to his Holy Prophet (P.B.U.H) who is forever a torch of guidance and knowledge for me.

Needless to say, about the distinguished and outstanding supervisor **Dr. Khadija Maqbol** who has helped the most important and pivotal role during my academic journey. Her pains-taking supervision and challenging queries were absolutely necessary to my research work. She has been much more than a supervisor, so again are my sincere thanks for the guidance, inspiration and unabated vigor to her.

Finally, I owe my profound gratitude to my parents **Abdur Rehman** and **Fozia** for their mellifluous affections, and to my brother **Khaliq Uz Zaman** for remembering me in their prayers. Which heaten me to achieve success in every sphere of my life and encouraged me throughout the span of study.

Javeria Javed

Contents

1	Fun	damental Concepts 5	5
		1.0.1 Fluid	5
		1.0.2 Fluid Mechanics	5
	1.1	Types of Flow	ó
		1.1.1 Laminar vs Turbulent Flow	5
		1.1.2 Steady vs Unsteady Flow	3
		1.1.3 Compressible vs Incompressible Flow	3
		1.1.4 Creeping vs Non-Creeping Flow	3
	1.2	Types of Fluid	3
		1.2.1 Newtonian vs Non-Newtonian Fluid	3
	1.3	Synovial fluid	7
		1.3.1 Types of Synovial fluid	7
	1.4	Fluid models and Synovial fluid	3
	1.5	Synovial fluid as a Couple Stress Fluid	3
	1.6	Permeability in Synovial membrane	3
	1.7	Flow Geometry and its Types)
		1.7.1 Permeable vs Non-Permeable Cavity)
		1.7.2 Reabsorption and its Types)
	1.8	Type of Boundary Conditions)
		1.8.1 Dirichlet Boundary Conditions)
		1.8.2 Neuman Boundary Condition	L
		1.8.3 Convective Boundary Condition 11	1

	1.9	Basic Laws of Fluid Mechanics	11
		1.9.1 Law of Conservation of Mass	11
		1.9.2 Law of Conservation of Momentum	12
	1.10	Series solution method	12
2	Mat	thematical study of synovial fluid using a Newtonian fluid model	14
	2.1	Introduction	14
	2.2	Mathematical Formulation	14
	2.3	Non-dimensional Quantities	17
	2.4	Solution of the Problem	18
	2.5	Results and Discussion	21
	2.6	Effect of Re-absorption rate V_0 :	21
		2.6.1 Effect of Periodicity Parameter α :	22
		2.6.2 Effect of Initial Flow Rate Q_0 :	22
		2.6.3 Effect of Axial position on Velocities:	23
	0.7	Conclusion	05
	2.7	Conclusion	25
3		thematical study of Synovial Fluid through a Knee Joint using a couple	25
3	Mat		25 27
3	Mat	thematical study of Synovial Fluid through a Knee Joint using a couple	
3	Mat stre	thematical study of Synovial Fluid through a Knee Joint using a couple	27
3	Mat stre	thematical study of Synovial Fluid through a Knee Joint using a couple ess fluid model Introduction	27 27
3	Mat stre	thematical study of Synovial Fluid through a Knee Joint using a couple ess fluid model Introduction	27 27 27 31
3	Mat stre 3.1 3.2	thematical study of Synovial Fluid through a Knee Joint using a couple ess fluid model Introduction	27 27 27 31
3	Mate stree 3.1 3.2 3.3	thematical study of Synovial Fluid through a Knee Joint using a couple ess fluid model Introduction	27 27 27 31 32
3	Mate stree 3.1 3.2 3.3	thematical study of Synovial Fluid through a Knee Joint using a couple ess fluid model Introduction	27 27 27 31 32 35
3	Mate stree 3.1 3.2 3.3	thematical study of Synovial Fluid through a Knee Joint using a couple ess fluid model Introduction	27 27 27 31 32 35 36
3	Mate stree 3.1 3.2 3.3	thematical study of Synovial Fluid through a Knee Joint using a couple ess fluid model Introduction	27 27 27 31 32 35 36 36
3	Mate stree 3.1 3.2 3.3	thematical study of Synovial Fluid through a Knee Joint using a couple ess fluid model Introduction Mathematical Formulation 3.2.1 Non-dimensional Quantities Solution of the Problem Result and Discussion 3.4.1 Effect of Reabsorption Parameter V_0 : 3.4.2 Effect of Couple-Stress Parameter λ : 3.4.3 Effect of Periodicity Parameter α :	27 27 27 31 32 35 36 36 37
3	Mate stree 3.1 3.2 3.3	thematical study of Synovial Fluid through a Knee Joint using a couple ess fluid model Introduction	27 27 27 31 32 35 36 36 37

Preface

Synovial fluid (SF) plays a crucial role in joint lubrication, reducing cartilage friction for smooth movement. It is located near the synovial membrane (SM), which consists of collagens, proteins, and proteoglycans key components influencing SF viscosity. The selectively permeable SM allows the absorption and secretion of SF, regulating water balance to prevent joint swelling (effusion) or inadequate lubrication, which may lead to joint damage. Several studies have examined SF flow characteristics. Yin et al. [1] highlighted the complexity of SF as a filtrate of interstitial fluids. Lai et al. [2] noted that SF flow depends on shear stress and deformation rate, but no single fluid model accurately describes its rheology. Ouerfelli et al. [3] emphasized the role of hyaluronic acid (HA) in joint lubrication, where SF behaves as a non-Newtonian fluid, shifting to Newtonian behavior after hyaluronidase treatment in osteoarthritis. Singh et al. [4] explored SF for arthritis treatment, while Hasnain et al. [5] modeled SF as a power-law fluid incorporating permeability and magnetic field effects. Magbool et al. [6, 7] analyzed SF flow through permeable conduits using the Linear Phan-Thien-Tanner (LPTT) model and found that periodic filtration influences pressure and velocity distribution. The viscosity of SF is determined by HA concentration, and its long-chain molecules can be modeled as a polar fluid. Rumanian et al. [8-9] used the couple-stress fluid model to study the hydrodynamic lubrication, noting the presence of couple stresses in fluids with large molecular structures. Previous studies [10-15] analyzed couple-stress effects in various flow conditions but did not consider SF as a couple-stress fluid.

The geometry of a flow system plays a key role in determining fluid behavior, tube-like geometries with circular cross-sections offer clear advantages by promoting smooth, uniform flow, minimizing friction, and maintaining laminar conditions. In comparison, slit or rectangular channels often produce higher shear stress at the edges, leading to flow separation, turbulence, and increased resistance. The symmetry and smooth surface of tubes reduce boundary effects and allow more balanced pressure distribution, resulting in lower energy losses and improved flow performance. Several studies have highlighted the benefits of tube-like geometries in fluid flow analysis. Pozrikidis et al. [16] developed an integral equation method specifically for studying Stokes flow in tubular structures. Shankar et al. [17] examined the stability of flow in both tubes and channels. Subsequent research by Siddiqui et al. [18-19], Maiti et al. [20],

Jeong J.T. et al. [21], and Farooq et al. [22] explored biological fluid flow through tubes and consistently demonstrated superior performance compared to flow in rectangular channels. Most recently, Hakligor et al. [23] investigated wake patterns behind permeable circular cylinders, showing that porosity significantly influences vortex behavior in tube-like geometries, crucial for optimizing fluid transport designs. Keeping in view the past study the present thesis is presented in following manner.

Chapter one describe the preliminaries, chapter two is the review work of siddiqui et al. [19], he has considered the bi-directional synovial fluid (Newtonian fluid) flow across the tube and discussed the flux and pressure of the fluid with in a tube. Chapter three is extended for the couple stress fluid flow with in a tube geometry and rheology of synovial fluid is analyzed by the couple stress fluid model with in a tube and near its boundary using the periodic filtration near the boundary.

Chapter 1

Fundamental Concepts

This chapter covers the fundamental concepts and definitions of fluid mechanics.

1.0.1 Fluid

A fluid is any substance that deforms under shearing forces and encompasses liquids, gases, and plasma.

1.0.2 Fluid Mechanics

Fluid mechanics is the study of behavior and motion of fluids, focusing on the forces acting on them and their properties such as pressure and flow.

1.1 Types of Flow

Flow can be classified on the basis of flow structure.

1.1.1 Laminar vs Turbulent Flow

Laminar flow refers to a pattern of fluid flow where all fluid particles follow a certain path and move smoothly without crossing each other. On the other hand, turbulent flow is distinguished by fluid particles that do not follow a specific path.

1.1.2 Steady vs Unsteady Flow

In steady flow, fluid properties such as velocity, pressure and density do not depend on time during flow, while in unsteady fluid flow properties changes with respect to time.

1.1.3 Compressible vs Incompressible Flow

Compressible flow encounters a remarkable change in density with varying pressure, temperature, and space variables. On contrary incompressible flow have a density that does not change with respect to space variables, pressure and temperature.

1.1.4 Creeping vs Non-Creeping Flow

In creeping flow frictional forces are outweighed by viscous force, such flows occur when fluid move very slowly or when it flows through very small channels. Whereas, non-creeping flow describes the flow behavior where inertial forces are dominant compared to viscous forces such flows occur at higher Reynolds numbers.

1.2 Types of Fluid

Fluid flow can be observed by different types of fluids, each with their own unique characteristics and behavior. These are classified as Newtonian and Non-Newtonian fluids.

1.2.1 Newtonian vs Non-Newtonian Fluid

A Newtonian fluid is that which exhibits a linear relationship between shear stress and velocity gradient whereas, non-Newtonian fluid do not adhere this relationship. Mathematically, shear stress and deformation rate are related by the following relation:

$$\tau_{rz} = \mu \gamma, \tag{1.1}$$

where μ is the coefficient of viscosity, γ is the rate of strain, and τ_{rz} is the shear stress.

Whereas for non-Newtonian fluid shear stress and deformation rate are related by the following non-linear relation:

$$\tau_{rz} = \eta \left(\gamma \right)^{n-1}. \tag{1.2}$$

where γ is the shear rate across adjacent fluid layers, n is the flow behavior index, and η represent the apparent viscosity that indicates the fluid's resistance to flow under particular conditions. Different non-Newtonian fluids models are power law model, viscoelastic model, Casson model and couple stress fluid model.

Couple Stress Fluid Model

It is a type of non-Newtonian fluid that undergoes additional internal forces to the particle's interaction with each other. Examples of couple stress fluids includes synovial fluid in knee and hip joints, blood flow in capillaries and arteries and lubricants in fluid machines.

1.3 Synovial fluid

Synovial fluid is a biological fluid having non-Newtonian nature because its viscosity varies due to stress and strain. It is present in synovial joints and work as a lubricants and reduces. Friction between cartilage during movements. To model the synovial fluid flow, the concepts of fluid flow, rheology, lubrication theory and biomechanics are required.

1.3.1 Types of Synovial fluid

The synovial fluid are classified as normal and inflammatory synovial fluid according to viscosity.

Normal Synovial fluid

In healthy human synovial fluid has high viscosity due to the composition of hyaluronic acid, lubricating protein and water. The shear thinning and pseudoplastic fluids can be considered as normal synovial fluid because it has pronounced shear thinning and viscoelasting behavior. The normal synovial fluid provides excellent joint lubrication because it is rich in hyaluronic acid and lubricating proteins.

Inflammatory Synovial fluid

In diseased condition inflammatory synovial fluid can be observed with low viscosity and less shear thinning property. The inflammatory synovial fluid as diluted hyaluronic acid with weak elasticity due to dilution. The inflammatory synovial fluid can be model using the Newtonian fluid model. Inflammatory synovial fluid can cause joints pain, stiffness of joints and swelling near the joints, also during movement such type of fluid causes pain and discomfort.

1.4 Fluid models and Synovial fluid

The synovial fluid are modeled on the basis of normal and inflammatory conditions, the most common model for normal synovial fluid are viscoelastic and shear thinning fluid. Its complicated rheological behavior includes time dependent stress relaxation and decreasing viscosity with increasing shear rate which is simulated by Maxwell fluid model, Oldroyd-B fluid model, Power law model, Second grade fluid model and Couple stress fluid model.

1.5 Synovial fluid as a Couple Stress Fluid

The microstructural and viscoelastic properties of synovial fluid, which are not well captured by traditional Newtonian or generalized Newtonian models, can be included by modeling it as a couple stress fluid. This model accounts micro-rotational effects in fluid and couple stresses resulting from the presence of long-chain hyaluronic acid and other micromolecules within the fluid. These elements provide extra resistance to deformation, which is crucial for lubricating cartilage surfaces, especially in small joint spaces or in low shear situations. Furthermore, couple stress theory offers a more precise description of fluid behavior in narrow or curved joint geometries such as those found in the knee, hip, or fingers where microscale interactions significantly influence flow dynamics.

1.6 Permeability in Synovial membrane

The synovial membrane's permeability is the capacity of the membrane to permit the passage of gases, nutrients, waste products, and compounds. Maintaining the composition of synovial fluid,

which lubricates and nourishes cartilage, is especially crucial for maintaining joint homeostasis.

1.7 Flow Geometry and its Types

External flow

Fluid flow around a body immersed in the fluid, where the boundary layer is free to develop in one direction. Examples include flow over a flat plate, around a cylinder, sphere, or airfoil.

Internal flow

Fluid flow that is completely confined within solid boundaries, such as flow through pipes, between parallel plates (duet flow), within annular spaces, or inside cavities.

1.7.1 Permeable vs Non-Permeable Cavity

A permeable cavity refers to a structure that allows the passage of fluid (liquids or gases) through its walls. Similar to a permeable cylinder, the material of the cavity has a porous structure that enables the movements of substances through it. Whereas, a non-permeable cavity is a type of cavity that prevents the passage of fluid through its walls. Some common example of non-permeable cavities are metal pipe, plastic syringes, and duets that are used for the transportation of substances without leakage.

1.7.2 Reabsorption and its Types

Constant Reabsorption

In constant reabsorption, a fixed percentage or amount of a substance is reabsorbed, regardless of its concentration in the filtrate. This process is not influenced by changes in concentration or volume and tends to be stable, steady mechanism. Mathematically velocity at the boundary is represented as follows:

$$V\left(R,z\right) = V_0. \tag{1.3}$$

Linear Reabsorption

In linear reabsorption, the rate of reabsorption increases proportionally with the concentration or volume of the substance in the filtrate. This means that as the amount of a substance in the filtrate rises, the reabsorption rate also increases, often in direct proportion. Mathematically velocity at the boundary is described as follows:

$$V(R,z) = V_0 + V_1 z. (1.4)$$

Periodic Reabsorption

In periodic reabsorption, the rate of reabsorption occurs in intervals or cycles with respect to the concentration or volume of the substance in the filtrate. This means that even as the amount of a substance in the filtrate rises, the reabsorption happens at specific times or phases. Mathematically velocity at the boundary is described as follows:

$$V(R,z) = V_0 \cos(\alpha z), \qquad (1.5)$$

$$V(R,z) = V_0 \sin(\alpha z). \tag{1.6}$$

1.8 Type of Boundary Conditions

There exist three primary types of boundary conditions.

1.8.1 Dirichlet Boundary Conditions

This boundary conditions specifies the value of unknown instead of its derivative at the boundary. The non-slip conditions indicates that the fluid's velocity at the boundary is equal to the velocity of the surface. For a stationary surface, this mean the fluid's velocity at the boundary is zero.

$$u(x,t) = g(x,t)$$
 on $\partial\Omega$. (1.7)

1.8.2 Neuman Boundary Condition

Neuman boundary condition is a type of boundary condition that specifies the derivative of the solution function at the domain's boundary. In fluid mechanics, a slip boundary condition sets the tangential velocity gradient at the boundary, when fluid doesn't cling to the surface.

$$\frac{\partial u}{\partial n}(x,t) = h(x,t)$$
 on $\partial\Omega$. (1.8)

1.8.3 Convective Boundary Condition

A convective boundary condition, or mixed boundary condition, is a combination of fixed value and flux that defines both the value of a function and it's derivative at the boundary.

$$-k\frac{\partial u}{\partial n} = h\left(u - u_{\infty}\right) \quad \text{on} \quad \partial\Omega.$$
 (1.9)

1.9 Basic Laws of Fluid Mechanics

1.9.1 Law of Conservation of Mass

Mass conservation law describes that mass cannot be created or destroyed within a system, and is expressed through the continuity equation in fluid dynamics. Mathematically, it is defined as follows:

$$\frac{\partial \rho}{\partial t} + \boldsymbol{\nabla} \left(\rho \mathbf{v} \right) = 0, \tag{1.10}$$

in cylindrical coordinates, above equation can be written as follows:

$$\frac{\partial \rho}{\partial t} + \frac{1}{r} \frac{\partial}{\partial r} (r \rho v_r) + \frac{1}{r} \frac{\partial}{\partial \theta} (r \rho v_\theta) + \frac{\partial}{\partial z} (\rho v_z) = 0, \tag{1.11}$$

where t is the time, ρ is the density, v_r, v_θ and v_z are the radial, azimuthal and axial component of velocity respectively.

For incompressible flow, density is constant and above equation becomes

$$\frac{1}{r}\frac{\partial}{\partial r}(rv_r) + \frac{1}{r}\frac{\partial}{\partial \theta}(rv_\theta) + \frac{\partial}{\partial z}(v_z) = 0.$$
 (1.12)

1.9.2 Law of Conservation of Momentum

This law states that the total amount of momentum remains unchanged within system, but it can only be altered under the effect of forces. Mathematically, it can be defined as follows:

$$\rho \left(\frac{d\mathbf{v}}{dt} - \mathbf{f} \right) + \nabla p = \nabla \tau, \tag{1.13}$$

where \mathbf{v} is the velocity vector, t is the time, p denotes the hydrostatic pressure, $\boldsymbol{\tau}$ represents the Cauchy stress tensor, and \mathbf{f} , and denotes the body forces.

Radial component of Eq.(1.13) is given below:

$$\rho \left(\frac{\partial v_r}{\partial t} + v_r \frac{\partial v_r}{\partial r} + v_\theta \left(\frac{1}{r} \frac{\partial v_r}{\partial \theta} - \frac{v_\theta}{r} \right) + v_z \frac{\partial v_r}{\partial z} \right) + \frac{\partial \rho}{\partial r}$$

$$= -\mu \left(\frac{1}{r} \frac{\partial}{\partial r} \left(r \tau_{rr} \right) + \frac{1}{r} \frac{\partial \tau_{\theta r}}{\partial \theta} + \frac{\partial \tau_{zr}}{\partial z} - \frac{\tau_{\theta \theta}}{r} \right) + \rho f_r. \tag{1.14}$$

Azimuthal component takes the following form:

$$\rho \left(\frac{\partial v_{\theta}}{\partial t} + v_{r} \frac{\partial v_{\theta}}{\partial r} + v_{\theta} \left(\frac{1}{r} \frac{\partial v_{\theta}}{\partial \theta} + \frac{v_{r}}{r} \right) + v_{z} \frac{\partial v_{\theta}}{\partial z} \right) + \frac{1}{r} \frac{\partial \rho}{\partial \theta}$$

$$= -\mu \left(\frac{1}{r^{2}} \frac{\partial}{\partial r} \left(r^{2} \tau_{r\theta} \right) + \frac{1}{r} \frac{\partial \tau_{\theta\theta}}{\partial \theta} + \frac{\partial \tau_{z\theta}}{\partial z} + \frac{\tau_{\theta r} - \tau_{r\theta}}{r} \right) + \rho f_{\theta}. \tag{1.15}$$

Axial component of Eq.(1.13) takes the following form:

$$\rho \left(\frac{\partial v_z}{\partial t} + v_r \frac{\partial v_z}{\partial r} + v_\theta \left(\frac{1}{r} \frac{\partial v_z}{\partial \theta} \right) + v_z \frac{\partial v_r}{\partial z} \right) + \frac{\partial \rho}{\partial z}$$

$$= -\mu \left(\frac{1}{r} \frac{\partial}{\partial r} \left(r \tau_{rz} \right) + \frac{1}{r} \frac{\partial \tau_{\theta z}}{\partial \theta} + \frac{\partial \tau_{zz}}{\partial z} \right) + \rho f_z. \tag{1.16}$$

where p is the pressure, μ is the dynamic viscosity, f_r , f_{θ} , and f_z are the body forces in radial, azimuthal, and axial directions respectively.

1.10 Series solution method

The power series method is a powerful analytical technique used to obtain exact or approximate solutions to differential equations by expressing the unknown function as an infinite series. It

is particularly effective for linear differential equations with variable coefficients.

Assume the following sixth-order differential equation:

$$y^{(6)} = F\left(r, y, y', y'', y''', y^{(4)}, y^{(5)}\right). \tag{1.17}$$

We assume a power series solution of the form:

$$y(r) = \sum_{n=0}^{\infty} a_n r^n, \tag{1.18}$$

compute all required derivatives up to the sixth order:

$$y'(r) = \sum_{n=1}^{\infty} a_n n r^n - 1, \quad y''(r) = \sum_{n=2}^{\infty} a_n n (n-1) r^{n-2}, \dots$$

$$y^{(6)}(r) = \sum_{n=6}^{\infty} a_n n (n-1) \dots (n-5) r^{n-6}. \tag{1.19}$$

Substitute these expressions into Eq.(1.17). After substitution, group terms by powers of r^n and set the coefficient of each power to zero. This yields a recurrence relation between the coefficients a_n , a_{n-1} , a_{n-2} , Using this recurrence relation along with initial or known values (e.g. $a_0, a_1, ...$), all coefficients can be determined. After computing the coefficients, the solution takes the form of a power series:

$$y(r) = a_0 + a_1 r + a_2 r^2 + a_3 r^3 + \dots (1.20)$$

Thus, the sixth-order differential equation is solved using a power series representation.

Chapter 2

Mathematical study of synovial fluid using a Newtonian fluid model

2.1 Introduction

This chapter is a review work of Siddiqui et. al. [19], who presented the steady, incompressible, two-dimensional flow of a Newtonian fluid through a permeable tube of finite length L and radius R. The fluid reabsorption at the permeable wall is considered to be a periodic function of axial length and mathematical model represents the bi-harmonic equation which is solved using a no-slip boundary condition. Expressions for velocity profile, stream function, pressure distribution and shear stress at the wall are calculated by series solution method. The variation in shear stress, velocity profile, stream function and pressure distribution are analyzed through graphical representations.

2.2 Mathematical Formulation

Consider a two-dimensional axisymmetric stokes flow through a tube of radius R and length L, as illustrated in Fig. 2.1.

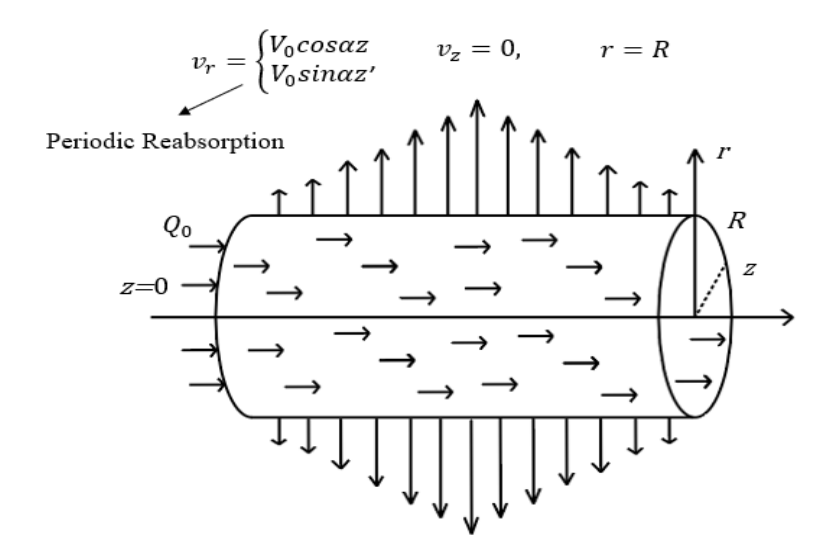


Fig. 2.1: Geometry of the flow

The symmetric nature of the flow along the centerline suggests the following velocity profile:

$$\mathbf{v} = (v_r(r, z), 0, v_z(r, z)), \qquad (2.1)$$

where $v_{r}\left(r,z\right)$ and $v_{z}\left(r,z\right)$ are the radial and axial velocity components, respectively.

To observe the flow properties, like velocity, pressure, and shear stress, following laws of fluid mechanics are used.

$$\nabla \cdot \mathbf{v} = 0, \tag{2.2}$$

$$\rho \left(\frac{\partial}{\partial t} + (\mathbf{v} \cdot \nabla) \right) \mathbf{v} + \nabla p = -\mu \nabla^2 \mathbf{v}, \tag{2.3}$$

where \mathbf{v} is the velocity vector, p is the hydrostatic pressure of the fluid, ρ is the fluid density, μ is the viscosity coefficient of Newtonian fluid. To find $\nabla^2 \mathbf{v}$, we used the vector identity $\nabla^2 \mathbf{v} = \nabla \times (\nabla \times \mathbf{v})$ and its expression is given as follows:

$$\nabla^2 \mathbf{v} = \left(-\frac{\partial}{\partial z} \left(\frac{\partial v_r}{\partial z} - \frac{\partial v_z}{\partial r} \right), 0, \frac{1}{r} \frac{\partial}{\partial r} \left(r \left(\frac{\partial v_r}{\partial z} - \frac{\partial v_z}{\partial r} \right) \right) \right). \tag{2.4}$$

Since the aim is to analyze creeping flow, the inertial term can be disregarded.

The component form of Eq. (2.2) - (2.3) for axisymmetric, incompressible Stokes flow takes the following form:

$$\frac{1}{r}\frac{\partial}{\partial r}(rv_r) + \frac{\partial}{\partial z}(v_z) = 0, \tag{2.5}$$

$$\frac{\partial p}{\partial r} = \mu \left(\frac{\partial}{\partial z} \left(\frac{\partial v_r}{\partial z} - \frac{\partial v_z}{\partial r} \right) \right), \tag{2.6}$$

$$\frac{\partial p}{\partial z} = -\mu \left(\frac{1}{r} \frac{\partial}{\partial r} \left(r \left(\frac{\partial v_r}{\partial z} - \frac{\partial v_z}{\partial r} \right) \right) \right), \tag{2.7}$$

and shear stress for axisymmetric flow is mentioned as follows:

$$\tau_{rz} = \mu \left(\frac{\partial v_r}{\partial z} - \frac{\partial v_z}{\partial r} \right). \tag{2.8}$$

The axisymmetric flow at the center of the tube meets the following boundary conditions:

$$v_r = 0, \frac{\partial v_z}{\partial r} = 0, \text{ at } r = 0.$$
 (2.9)

The periodic reabsorption rate and no-slip conditions at the permeable wall of the tube satisfy the following boundary conditions:

$$v_r = \begin{cases} V_0 \sin \alpha z \\ V_0 \cos \alpha z \end{cases} \quad \text{at} \quad r = R,$$

$$v_z = 0$$
, at $r = R$.

The fluid enters into the system with a linear flow rate and fulfills the above mentioned boundary conditions at the entry region z = 0

$$Q_0 = 2\pi \int_{0}^{R} r v_z(r, 0) dr$$
, at $z = 0$.

The set of Eqs. (2.6) - (2.7) represent the linear partial differential equation in which three unknown v_r, v_z and p are involved. We will cross differentiate Eqs. (2.6) - (2.7) to eliminate the pressure gradient in the following form:

$$\mu\left(\frac{\partial}{\partial z}\left(\frac{\partial}{\partial z}\left(\frac{\partial v_r}{\partial z} - \frac{\partial v_z}{\partial r}\right)\right) - \frac{\partial}{\partial r}\left(\frac{1}{r}\frac{\partial}{\partial r}\left(r\left(\frac{\partial v_r}{\partial z} - \frac{\partial v_z}{\partial r}\right)\right)\right)\right) = 0. \tag{2.10}$$

To reduce the number of unknowns, following relation of stream function will be used.

$$v_r = \frac{1}{r} \frac{\partial \psi}{\partial z}, \quad v_z = -\frac{1}{r} \frac{\partial \psi}{\partial r}.$$
 (2.11)

Inserting above form of stream function in Eq. (2.10), one can get the following form of equation:

$$\mu\left(\nabla^2\left(\frac{1}{r}E^2\psi\right) - \frac{1}{r^2}\left(\frac{1}{r}E^2\psi\right)\right) = 0,\tag{2.12}$$

where

$$\nabla^2 = \left(\frac{\partial^2}{\partial r^2} + \frac{1}{r}\frac{\partial}{\partial r} + \frac{\partial^2}{\partial z^2}\right),\tag{2.13}$$

and

$$E^{2} = \left(\frac{\partial^{2}}{\partial r^{2}} - \frac{1}{r}\frac{\partial}{\partial r} + \frac{\partial^{2}}{\partial z^{2}}\right). \tag{2.14}$$

After performing further calculations in Eq.(2.12), we can get the fourth order linear homogeneous PDE in the following form:

$$E^{4}(\psi) = 0. (2.15)$$

The boundary condition in term of the stream function are expressed as follows:

$$\frac{\partial}{\partial r} \left(-\frac{1}{r} \frac{\partial \psi}{\partial r} \right) = 0, \quad \frac{1}{r} \frac{\partial \psi}{\partial z} = 0 \quad \text{at} \quad r = 0,$$

$$-\frac{1}{r} \frac{\partial \psi}{\partial r} = 0, \quad \frac{1}{r} \frac{\partial \psi}{\partial z} = \begin{cases} V_0 \sin \alpha z \\ V_0 \cos \alpha z \end{cases} \quad \text{at} \quad r = R,$$

$$\frac{Q_0}{2\pi} = \psi (0, 0) - \psi (R, 0) \quad \text{at} \quad z = 0.$$
(2.16)

2.3 Non-dimensional Quantities

For non-dimensional analysis following quantities are defined:

$$r' = \frac{r}{R}, \ z' = \frac{z}{R}, \ v_{r'} = \frac{v_r}{V_1}, \ v_{z'} = \frac{v_z}{V_1}, \ Q'_0 = \frac{Q_0}{V_1 R^2},$$
 (2.17)

$$V_0^{'} = \frac{V_0}{V_1}, \ p^{'} = \frac{p}{\mu V_1 R}, \ \psi^{'} = \frac{\psi}{V_1 R^2}.$$

The dimensionless form of Eq. (2.15) - (2.16) takes the following form:

$$E^{4}(\psi) = 0, (2.18)$$

$$\frac{\partial}{\partial r} \left(-\frac{1}{r} \frac{\partial \psi}{\partial r} \right) = 0, \quad \frac{1}{r} \frac{\partial \psi}{\partial z} = 0 \quad \text{at} \quad r = 0,$$

$$-\frac{1}{r} \frac{\partial \psi}{\partial r} = 0, \quad \frac{1}{r} \frac{\partial \psi}{\partial z} = \begin{cases} V_0 \sin \alpha z \\ V_0 \cos \alpha z \end{cases} \quad \text{at} \quad r = 1,$$

$$\frac{Q_0}{2\pi} = \psi (0, 0) - \psi (R, 0) \quad \text{at} \quad z = 0.$$
(2.19)

2.4 Solution of the Problem

To solve the linear fourth order PDE, we will assume an inverse method and the exact solution of Eq.(2.18) can be obtained by defining the following stream function $\psi(r, z)$

$$\psi(r, z) = (\cos \alpha z) F(r) + G(r).$$

Similarly, when the reabsorption of the wall is cosine function Eq.(2.18) can be solved by using the following stream function $\psi(r, z)$.

$$\psi(r,z) = (\sin \alpha z) F(r) + G(r), \qquad (2.21)$$

where F(r) and G(r) are functions that are unknown.

Using above solution in Eq. (2.15), one can get the following systems of ODE's:

$$L_{1}^{4}F\left(r\right) =0, \tag{2.22}$$

$$E_{1}^{4}G\left(r\right) =0, \tag{2.23}$$

where

$$L_1^2 = \left(\frac{d^2}{dr^2} - \frac{1}{r}\frac{d}{dr} - \alpha^2\right),\tag{2.24}$$

and

$$E_1^2 = \left(\frac{d^2}{dr^2} - \frac{1}{r}\frac{d}{dr}\right). {(2.25)}$$

The associated boundary conditions are as follows:

$$F = 0, \quad \frac{d}{dr} \left(\frac{1}{r} \frac{dF}{dr} \right) = 0, \quad \text{at} \quad r = 0,$$
 (2.26)

$$\frac{1}{r}\frac{dF}{dr} = 0, \quad F = \frac{-V_0}{\alpha} \quad \text{at} \quad r = 1,$$

$$G = 0, \quad \frac{d}{dr}\left(\frac{1}{r}\frac{dG}{dr}\right) = 0, \quad \text{at} \quad r = 0,$$

$$\frac{d}{dr}\left(\frac{1}{r}\frac{dG}{dr}\right) = 0, \quad \text{at} \quad r = 1,$$

$$G(R) - G(0) = \frac{-Q_0}{2\pi} - (F(R) - F(0)), \quad \text{at} \quad z = 0.$$

$$(2.27)$$

The solution of Eq.(2.22) can be represented as follow as mentioned in Ref. [19]

$$\left(\frac{d^2}{dr^2} - \frac{1}{r}\frac{d}{dr} - \alpha^2\right)^2 F(r) = 0,$$
(2.28)

$$F(r) = r(c_1 I_1(\alpha r) + c_2 K_1(\alpha r) + r(c_3 I_2(\alpha r) + c_4 K_2(\alpha r))), \qquad (2.29)$$

where I_1 and I_2 represent modified Bessel function of first kind, K_1 and K_2 are modified bessel function of second kind. For bounded solution B.c's (2.26) implies $c_2 = c_4 = 0$ leading to the following finite solution:

$$F(r) = r\left(c_1 I_1\left(\alpha r\right) + r c_3 I_2\left(\alpha r\right)\right). \tag{2.30}$$

Now with the help of remaining boundary conditions, find the values of c_1 and c_3 , which can be listed in appendix. The final solution of F(r) becomes:

$$F(r) = \frac{r(-I_1(\alpha)I_1(\alpha r) + rI_0(\alpha)I_2(\alpha r))V_0}{-\alpha I_0^2(\alpha) + 2I_0(\alpha)I_1(\alpha) + \alpha I_1^2(\alpha)}.$$
 (2.31)

To find the solution of G(r), solve the following equation:

$$\left(\frac{d^2}{dr^2} - \frac{1}{r}\frac{d}{dr}\right)^2 G(r) = 0, \tag{2.32}$$

where

$$\left(\frac{d^2}{dr^2} - \frac{1}{r}\frac{d}{dr}\right) = r\frac{d}{dr}\left(\frac{1}{r}\frac{d}{dr}\right),$$
(2.33)

Integrate both side of Eq.(2.32) one can get the following solution

$$G(r) = b_1 \frac{r^4}{16} + b_2 \frac{r^2}{2} \left(\ln r - \frac{1}{2} \right) + b_3 \frac{r^2}{2} + b_4, \tag{2.34}$$

Boundary condition at r = 0 suggest $b_2 = 0, b_3 = 0$.

Now Eq.(2.34) reduce into following follow

$$G(r) = b_1 \frac{r^4}{16} + b_3 \frac{r^2}{2},\tag{2.35}$$

remaining boundary conditions will get the following form of solution

$$G(r) = \frac{r^2 (2 - r^2) (2\pi v_0 - \alpha Q_0)}{2\pi \alpha}.$$
 (2.36)

After substituting F(r) and G(r) into Eq.(2.20). The stream function for the case of sinusoidal reabsorption takes the following form

$$\psi(r,z) = \frac{r(-I_{1}(\alpha)I_{1}(\alpha r) + rI_{0}(\alpha)I_{2}(\alpha r))V_{0}\cos(\alpha z)}{-\alpha I_{0}^{2}(\alpha) + 2I_{0}(\alpha)I_{1}(\alpha) + \alpha I_{1}^{2}(\alpha)} + \frac{r^{2}(2 - r^{2})(2\pi v_{0} - \alpha Q_{0})}{2\pi\alpha}.$$
(2.37)

Using above stream function in Eq.(2.11), one can get the following velocity components:

$$v_r = \frac{-\alpha \left(-I_1\left(\alpha\right)I_1\left(\alpha r\right) + rI_0\left(\alpha\right)I_2\left(\alpha r\right)\right)V_0\sin\left(\alpha z\right)}{-\alpha I_0^2\left(\alpha\right) + 2I_0\left(\alpha\right)I_1\left(\alpha\right) + \alpha I_1^2\left(\alpha\right)},\tag{2.38}$$

$$v_{z} = \frac{\alpha \left(-I_{1}\left(\alpha\right) I_{0}\left(\alpha r\right) + r I_{0}\left(\alpha\right) I_{1}\left(\alpha r\right)\right) V_{0} \cos\left(\alpha z\right)}{\alpha I_{0}^{2}\left(\alpha\right) - 2I_{0}\left(\alpha\right) I_{1}\left(\alpha\right) - \alpha I_{1}^{2}\left(\alpha\right)} + \frac{2\left(-1 + r\right)\left(1 + r\right)\left(2\pi v_{0} - \alpha Q_{0}\right)}{\pi \alpha}.$$

$$(2.39)$$

In a similar manner, substitute the solution F(r) and G(r) into Eq.(2.21). The stream function corresponding to the cosine function can be determined and is given as follows:

$$\psi(r,z) = \frac{r(-I_{1}(\alpha)I_{1}(\alpha r) + rI_{0}(\alpha)I_{2}(\alpha r))V_{0}\sin(\alpha z)}{-\alpha I_{0}^{2}(\alpha) + 2I_{0}(\alpha)I_{1}(\alpha) + \alpha I_{1}^{2}(\alpha)} + \frac{r^{2}(2 - r^{2})(2\pi v_{0} - \alpha Q_{0})}{2\pi\alpha}.$$
(2.40)

The velocity components can be derived using the above stream function in Eq.(2.11)

$$v_r = \frac{\alpha \left(-I_1\left(\alpha\right) I_1\left(\alpha r\right) + r I_0\left(\alpha\right) I_2\left(\alpha r\right)\right) V_0 \cos\left(\alpha z\right)}{-\alpha I_0^2\left(\alpha\right) + 2 I_0\left(\alpha\right) I_1\left(\alpha\right) + \alpha I_1^2\left(\alpha\right)},\tag{2.41}$$

$$v_{z} = \frac{\alpha \left(-I_{1}\left(\alpha\right) I_{0}\left(\alpha r\right) + r I_{0}\left(\alpha\right) I_{1}\left(\alpha r\right)\right) V_{0} \sin\left(\alpha z\right)}{\alpha I_{0}^{2}\left(\alpha\right) - 2 I_{0}\left(\alpha\right) I_{1}\left(\alpha\right) - \alpha I_{1}^{2}\left(\alpha\right)} + \frac{2\left(r^{2} - 1\right) \left(2\pi v_{0} - \alpha Q_{0}\right)}{\pi \alpha}.$$

$$(2.42)$$

2.5 Results and Discussion

To observe how emerging parameters effect the fluid flow, we have presented the graphical results in this section. The influence of periodic reabsorption velocity $V_0 \sin{(\alpha z)}$ and flux Q_0 is represented by radial and axial velocity, pressure distribution and shear stress at the wall.

2.6 Effect of Re-absorption rate V_0 :

The variation in radial velocity for different values of re-absorption parameter V_0 is shown in Fig. 2.2 (a). At the axis of the tube, the radial flow remains stationary, but it increases near the boundary due to nutrient re-absorption. This increase is more significant when the re-absorption follows a cosine profile compared to a sine profile Fig. 2.2 (b) illustrates the effect of V_0 on axial velocity. It is observed that axial flow increases as the re-absorption rate increases near the synovial membrane. The enhancement of axial flow is notably greater when the nutrient re-absorption follows a cosine distribution. Fig. 2.2(c) demonstrates that the pressure within the synovial fluid is influenced by the nutrient re-absorption rate. As V_0 increases, the internal

pressure in the synovial joint also rises. The pressure build-up is more pronounced with a cosine-type re-absorption, and the pressure gradient becomes steeper compared to the sine-type re-absorption Fig. 2.2(d) highlights the impact of nutrient re-absorption rate V_0 on wall shear stress. Higher re-absorption rates lead to increased shear forces near the synovium. The simulation indicates that when nutrient re-absorption follows a cosine profile, the shear forces are significantly stronger compared to those resulting from a sine-type re-absorption profile.

2.6.1 Effect of Periodicity Parameter α :

The influence of the periodicity parameter α on both radial and axial velocities for sine and cosine types of re-absorption rates is shown in Fig.2.3 (a–b). In both cases, an increase in α leads to a reduction in flow along the radial and axial directions. However, this deceleration is more significant for the cosine-type re-absorption compared to the sine-type. The decline in both axial and radial velocities is more pronounced when the nutrient re-absorption follows a cosine pattern Fig. 2.3 (c) demonstrates that an increase in the periodicity parameter results in greater load requirements for joint lubrication under both sine and cosine re-absorption conditions. The increased flow resistance makes the fluid more viscous, thereby requiring higher pressure for effective joint lubrication. This pressure buildup is more dominant in the case of cosine-type re-absorption than the sine-type. Lastly, Fig. 2.3 (d) illustrates the variation in wall shear stress with respect to the periodicity parameter α . It shows that lower values of α demand higher shear stress along the synovium. Furthermore, the shear forces are notably stronger when the nutrient re-absorption follows a cosine profile compared to a sine profile.

2.6.2 Effect of Initial Flow Rate Q_0 :

The impact of the flow rate Q_0 on axial velocity is illustrated in Fig.2.4 (a) for both sine and cosine re-absorption rate of nutrients. In the case of cosine re-absorption, the axial flow decreases, whereas for sine re-absorption, an increase in flow rate leads to an enhancement in axial velocity. Fig. 2.4 (b) shows that an increase in flow rate reduces the load required for joint lubrication in both sine and cosine re-absorption scenarios. However, the pressure generated within the joint is more pronounced for the cosine type of re-absorption compared to the sine type. Lastly, Fig. 2.4(c) presents the variation in wall shear stress with respect to the flow

rate Q_0 . It reveals that the fluid exerts higher shear stress along the synovium under sine re-absorption, while lower shear stress is observed for cosine re-absorption.

2.6.3 Effect of Axial position on Velocities:

Fig. 2.5 (a–b) illustrates the effect of axial position on both radial and axial velocities for cosine and sine types of nutrient re-absorption. In both cases, an increase in axial position results in a reduction in flow along both the radial and axial directions.

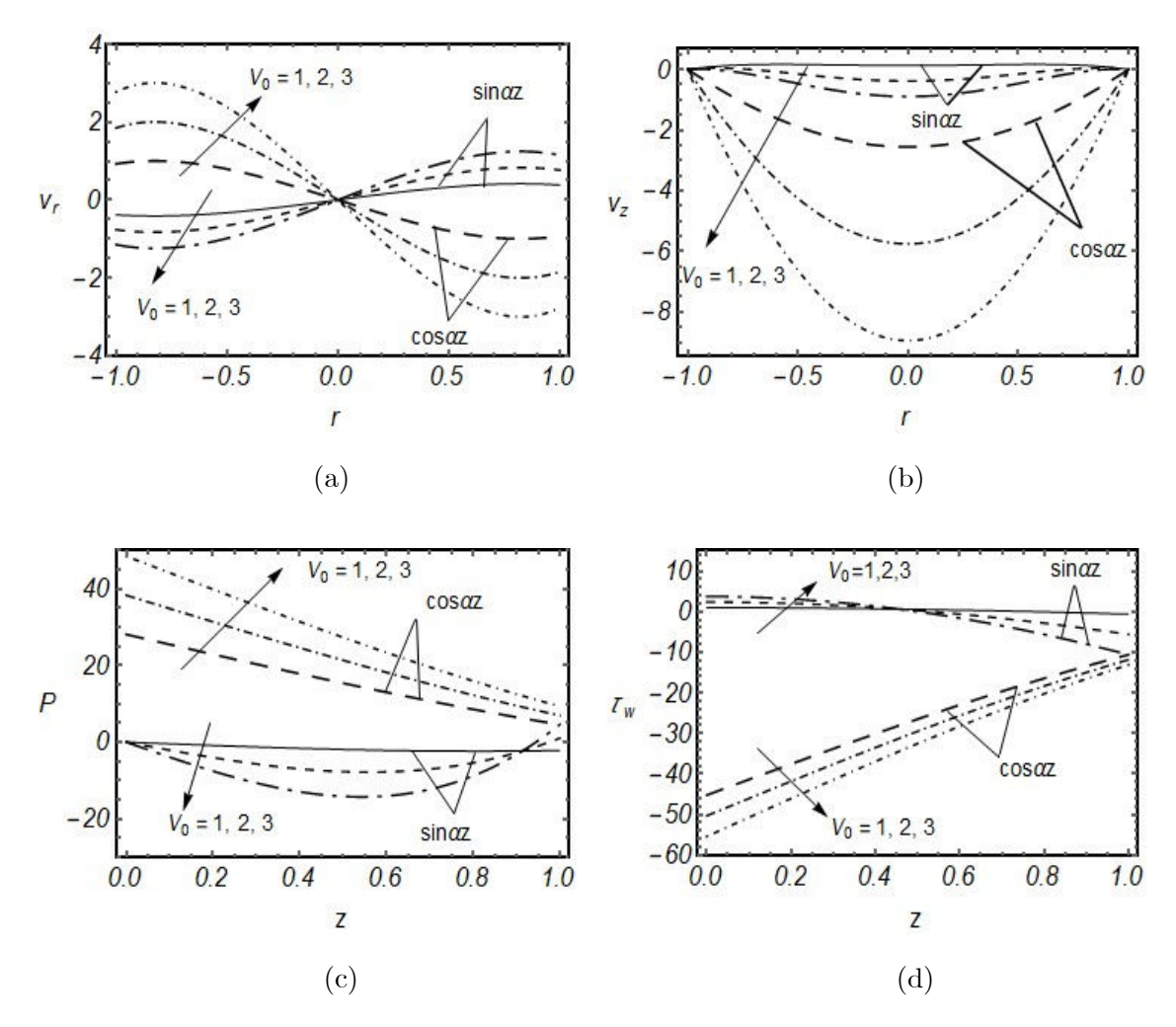


Fig. 2.2a (a-d): Influence of reabsorption parameter V_0 on (a) radial velocity (b) axial velocity (c) pressure distribution, and (d) wall shear stress.

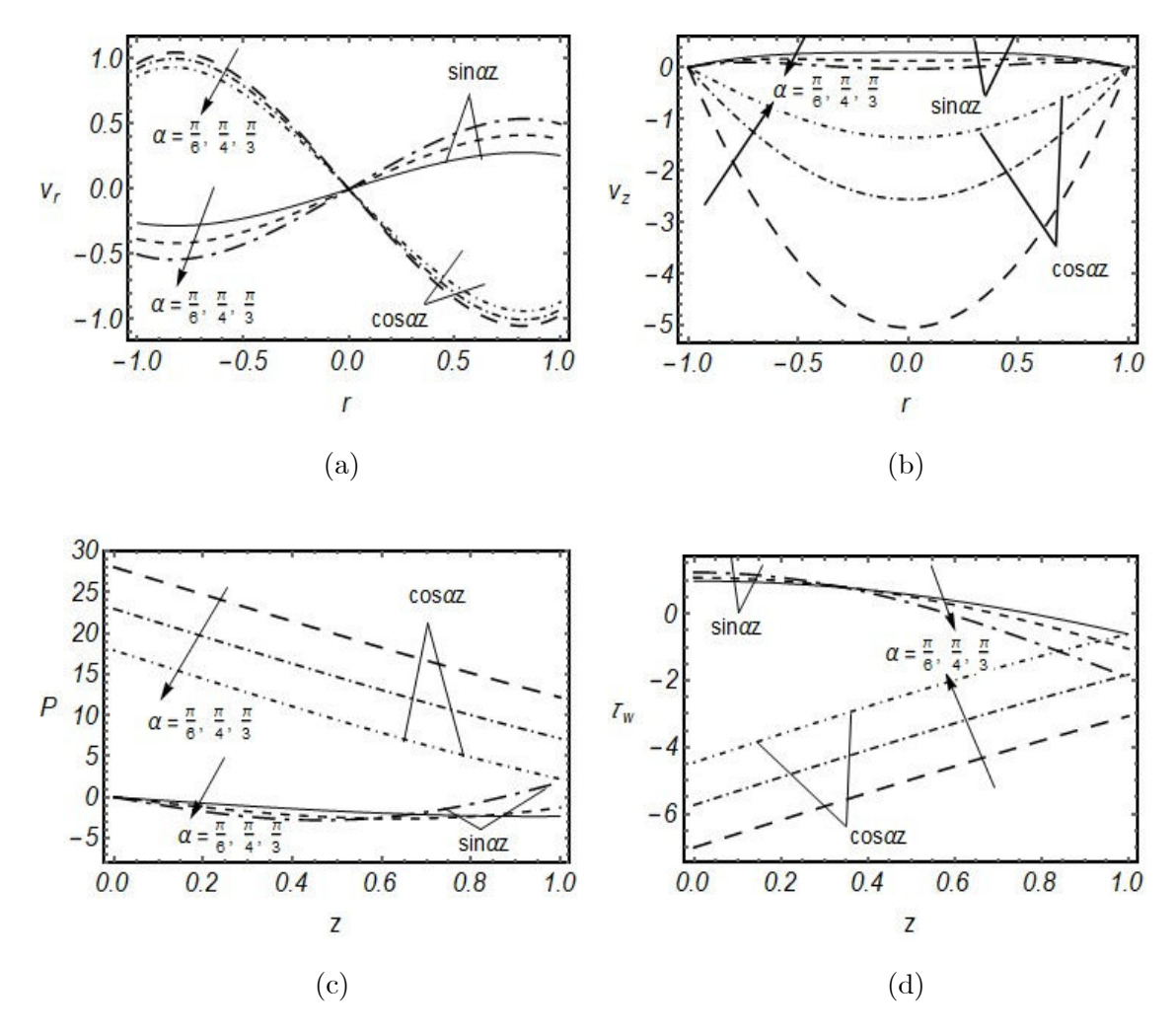
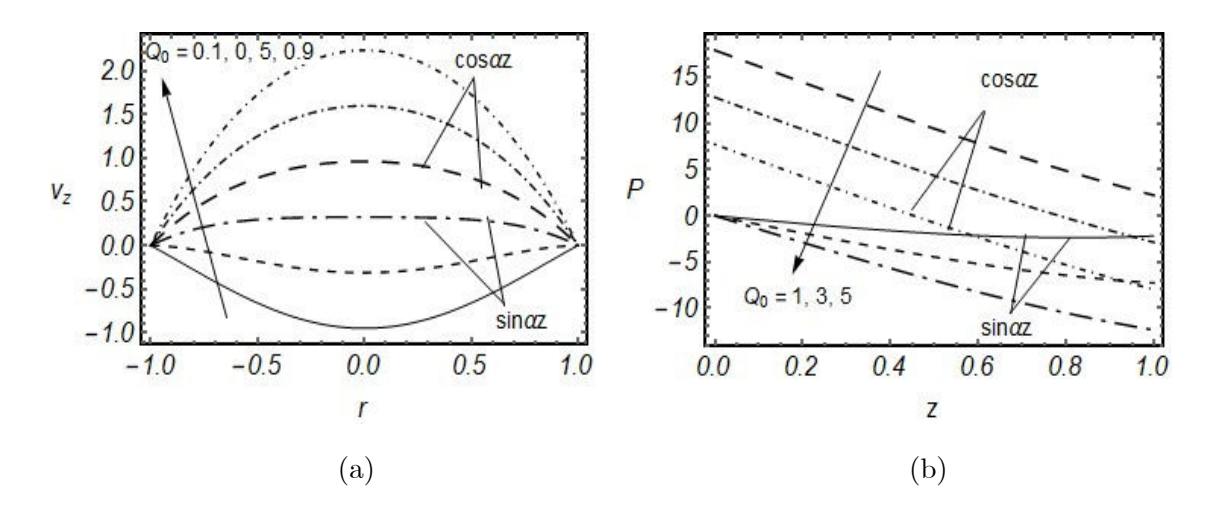


Fig.2.3a (a-d): Influence of periodicity parameter α on (a) radial velocity, (b) axial velocity, (c) pressure distribution, and (d) wall shear stress.



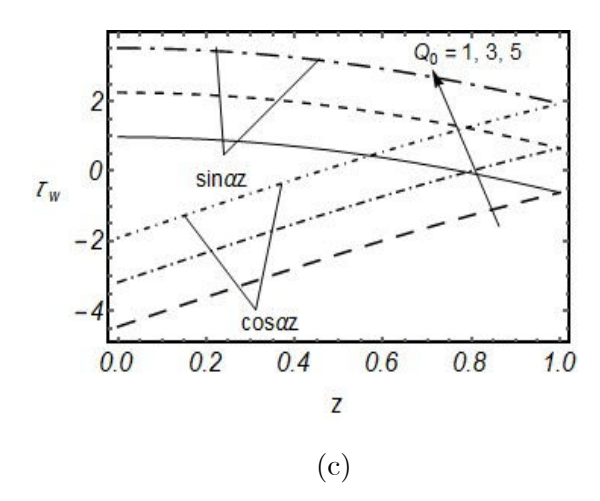


Fig. 2.4a (a-c): Influence of initial flow rate Q_0 on (a) axial velocity, (b) pressure distribution, and (c) wall shear stress.

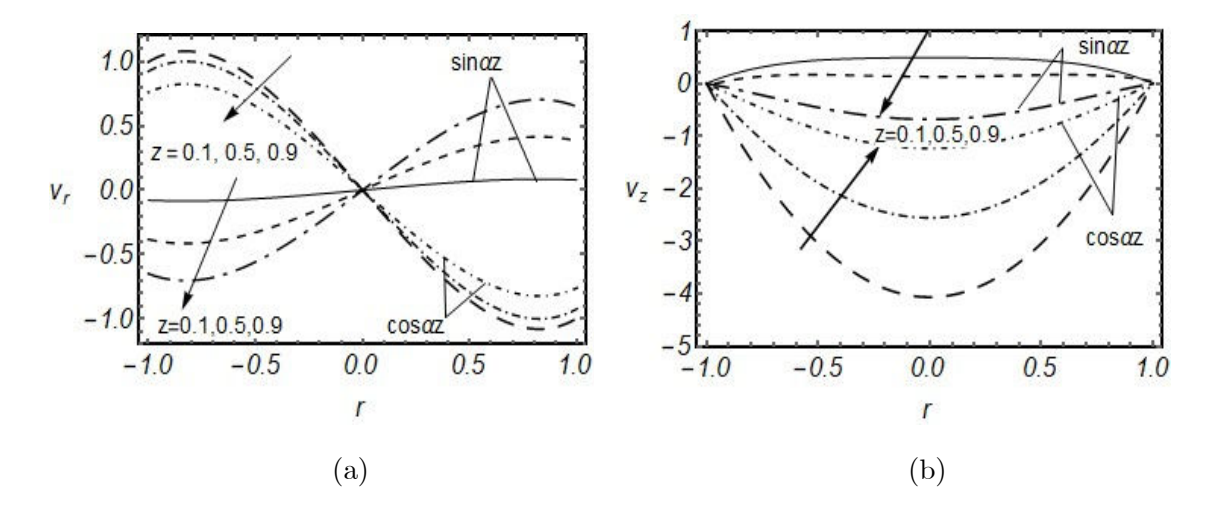


Fig.2.5a (a-b): Variation in axial and radial velocity at entry, middle and exit region of the tube.

2.7 Conclusion

This study offers a comprehensive understanding of shear forces and load distribution in synovial fluid flow using a Newtonian fluid model. The analysis focuses on the slow movement of synovial fluid through the synovium, considering both sine and cosine types of nutrient re-absorption rates. It examines how these re-absorption patterns influence the flow behavior, shear stress,

and load within a knee joint filled with synovial fluid.

A mathematical model is developed based on the rheological properties of the fluid, governed by classical fluid mechanics principles. The simulations are carried out using Mathematica software. The results indicate that axial flow within the tube is more pronounced when nutrients are reabsorbed at a cosine-type rate compared to a sine-type rate. Similarly, radial flow is also enhanced under the cosine re-absorption condition. Furthermore, both load and shear stress within the synovial fluid increase significantly when the nutrient re-absorption follows a cosine pattern rather than a sine one.

This research contributes valuable insights for evaluating the flow characteristics and loadbearing capacity of synovial fluid in artificial knee joints.

Chapter 3

Mathematical study of Synovial Fluid through a Knee Joint using a couple stress fluid model

3.1 Introduction

This chapter extends the work of siddiqui presented in previous chapter, for an incompressible, two-dimensional, steady, creeping flow of couple stress fluid through a permeable tube of finite length L and radius R. The fluid reabsorption assumed to be periodic at the permeable wall of the tube, and no-slip boundary condition are used to solve the bi-harmonic equation. Expressions for velocity profile, stream function, pressure distribution and shear stress at the wall are calculated by series solution method. The variation in shear stress, velocity profile and pressure distribution is observed by graphs.

3.2 Mathematical Formulation

Consider two-dimensional axisymmetric flow of couple stress fluid through a tube of radius R and length L which is shown in Fig. 3.1. The two-dimensional creeping flow suggests that the z-axis along the length of the tube and the r-axis along its radial direction.

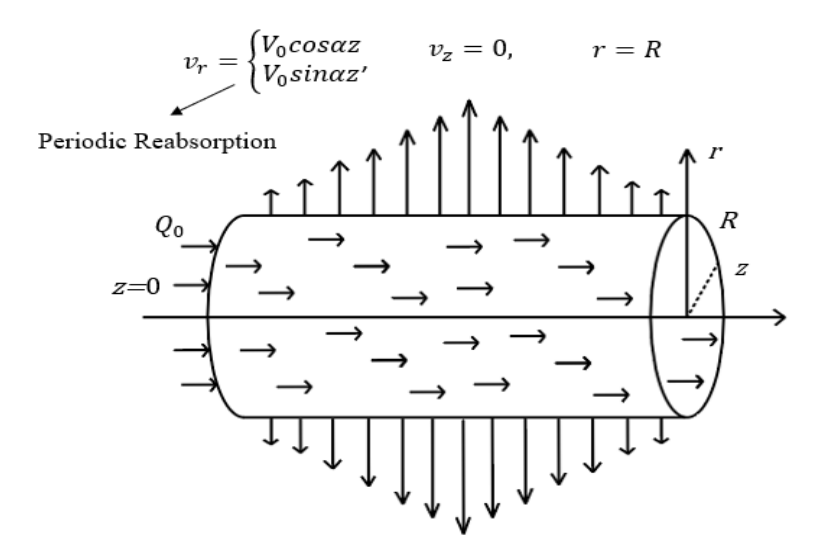


Fig.3.1: Geometry of the flow

The symmetric flow along the center line (z - axis) of the tube suggests the following velocity profile:

$$\mathbf{v} = (v_r(r, z), 0, v_z(r, z)), \tag{3.1}$$

where $v_r(r, z)$ and $v_z(r, z)$ are the radial and axial velocity components, respectively.

The two-dimensional, incompressible, creeping flow of couple stress fluid satisfy the following law of fluid mechanics

$$\nabla . \mathbf{v} = 0, \tag{3.2}$$

$$\rho \left(\frac{\partial}{\partial t} + (\nabla \cdot \mathbf{v}) \right) \mathbf{v} + \nabla p = -\mu \nabla^2 \mathbf{v} - \xi \nabla^4 \mathbf{v}, \tag{3.3}$$

where \mathbf{v} is the velocity, p is the hydrostatic pressure of the fluid, ρ is the density, μ is the coefficient of Newtonian fluid and ξ is the coefficient of couple stress fluid. The value of $\nabla^2 \mathbf{v}$ is given in Eq.(2.4) and to find $\nabla^4 \mathbf{v}$, we use the vector identity $\nabla^2 (\nabla^2 \mathbf{v}) = \nabla^4 \mathbf{v}$.

$$\nabla^{4}\mathbf{v} = \left(0, \frac{1}{r} \frac{\partial}{\partial z} \left(r \left(\frac{\partial}{\partial r} \left(\frac{1}{r} \frac{\partial}{\partial r} \left(r \left(\frac{\partial v_{r}}{\partial z} - \frac{\partial v_{z}}{\partial r}\right)\right)\right) + \frac{\partial^{2}}{\partial z^{2}} \left(\frac{\partial v_{r}}{\partial z} - \frac{\partial v_{z}}{\partial r}\right)\right)\right), 0\right).$$
(3.4)

The component form of Eq. (3.2) - (3.3) for axisymmetric, incompressible flow of couple stress fluid takes the following form:

$$\frac{1}{r}\frac{\partial}{\partial r}(rv_r) + \frac{\partial}{\partial z}(v_z) = 0, \tag{3.5}$$

$$\frac{\partial p}{\partial r} = \mu \left(\frac{\partial \Omega}{\partial z} \right) - \xi \left(\frac{1}{r} \frac{\partial}{\partial z} r \left(-\frac{\Omega}{r^2} + \frac{1}{r} \frac{\partial \Omega}{\partial r} + \frac{\partial^2 \Omega}{\partial r^2} + \frac{\partial^2 \Omega}{\partial z^2} \right) \right), \tag{3.6}$$

$$\frac{\partial p}{\partial z} = -\mu \left(\frac{1}{r} \frac{\partial}{\partial r} (r\Omega) \right) + \xi \left(\frac{1}{r} \frac{\partial}{\partial r} r \left(-\frac{\Omega}{r^2} + \frac{1}{r} \frac{\partial \Omega}{\partial r} + \frac{\partial^2 \Omega}{\partial r^2} + \frac{\partial^2 \Omega}{\partial z^2} \right) \right), \tag{3.7}$$

and shear stress for axisymmetric flow is given as follows:

$$\tau_{rz} = \mu\left(\Omega\right) - \xi\left(-\frac{\Omega}{r^2} + \frac{1}{r}\frac{\partial\Omega}{\partial r} + \frac{\partial^2\Omega}{\partial r^2} + \frac{\partial^2\Omega}{\partial z^2}\right),\tag{3.8}$$

where

$$\Omega = \frac{\partial v_r}{\partial z} - \frac{\partial v_z}{\partial r}.$$
(3.9)

The axisymmetric flow at the center of the tube meets the following boundary conditions:

$$v_r = 0, \quad \frac{\partial v_z}{\partial r} = 0, \text{ at } r = 0,$$
 (3.10)

The periodic reabsorption rate and non-slip condition at the permeable wall of the tube satisfy the following boundary conditions:

$$v_z = 0, \quad v_r = \begin{cases} V_0 \sin \alpha z \\ V_0 \cos \alpha z \end{cases}$$
 at $r = R$,

The absence of couple stress due to irrotational motion of fluid particles at the wall of the tube is described by the following boundary conditions:

$$\Omega = 0$$
, at $r = R$.

The couple stress fluid enters into the system with a contact flow rate and adhere the boundary

conditions listed below at the entry region z = 0.

$$Q_0 = 2\pi \int_{0}^{R} r v_z(r, 0) dr$$
, at $z = 0$.

Differentiating Eq. (3.6) w.r.t z and Eq. (3.7) w.r.t r to eliminate the pressure gradient, one can get the following form of equations:

$$\frac{\partial^2 p}{\partial r \partial z} = \mu \left(\frac{\partial^2 \Omega}{\partial z^2} \right) - \xi \frac{\partial}{\partial z} \left(\left(\frac{1}{r} \frac{\partial}{\partial z} r \left(-\frac{\Omega}{r^2} + \frac{1}{r} \frac{\partial \Omega}{\partial r} + \frac{\partial^2 \Omega}{\partial r^2} + \frac{\partial^2 \Omega}{\partial z^2} \right) \right) \right), \tag{3.11}$$

$$\frac{\partial^2 p}{\partial r \partial z} = -\mu \frac{\partial}{\partial r} \left(\left(\frac{1}{r} \frac{\partial}{\partial r} \left(r \Omega \right) \right) \right) + \xi \frac{\partial}{\partial r} \left(\left(\frac{1}{r} \frac{\partial}{\partial r} r \left(-\frac{\Omega}{r^2} + \frac{1}{r} \frac{\partial \Omega}{\partial r} + \frac{\partial^2 \Omega}{\partial r^2} + \frac{\partial^2 \Omega}{\partial z^2} \right) \right) \right). \tag{3.12}$$

Subtracting Eqs. (3.11) - (3.12), yields the following equation:

$$\mu\left(\mathbf{\nabla}^{2}\Omega - \frac{\Omega}{r^{2}}\right) - \xi\left(\left(\mathbf{\nabla}^{4}\Omega - \frac{\mathbf{\nabla}^{2}\Omega}{r^{2}}\right) - \frac{1}{r^{2}}\left(\mathbf{\nabla}^{2}\Omega - \frac{\Omega}{r^{2}}\right)\right) = 0,$$
(3.13)

where

$$\nabla^2 = \left(\frac{\partial^2}{\partial r^2} + \frac{1}{r}\frac{\partial}{\partial r} + \frac{\partial^2}{\partial z^2}\right). \tag{3.14}$$

Eq. (3.13) is the fifth order partial differential equation (PED) in two variables, which can be reduced into one variable by the following stream function:

$$v_r = \frac{1}{r} \frac{\partial \psi}{\partial z}, \quad v_z = -\frac{1}{r} \frac{\partial \psi}{\partial r}.$$
 (3.15)

Vorticity function Ω in term of stream function takes the following form:

$$\Omega = -\frac{1}{r}E^2\psi,\tag{3.16}$$

where

$$E^{2} = \left(\frac{\partial^{2}}{\partial r^{2}} - \frac{1}{r}\frac{\partial}{\partial r} + \frac{\partial^{2}}{\partial z^{2}}\right). \tag{3.17}$$

Eq. (3.13) in term of above stream function takes the following form:

$$\xi E^6 \psi - \mu E^4 \psi = 0, \tag{3.18}$$

where

$$E^{6} = E^{2}(E^{2}(E^{2})), E^{4} = E^{2}(E^{2}), (3.19)$$

and boundary conditions expressed in term of the stream function are provided below:

$$\frac{1}{r}\frac{\partial\psi}{\partial z} = 0, \quad \frac{\partial}{\partial r}\left(-\frac{1}{r}\frac{\partial\psi}{\partial r}\right) = 0 \quad \text{at} \quad r = 0,$$

$$-\frac{1}{r}\frac{\partial\psi}{\partial r} = 0, \quad \frac{1}{r}E^{2}\psi = 0, \quad \frac{1}{r}\frac{\partial\psi}{\partial z} = \begin{cases} V_{0}\sin\alpha z \\ V_{0}\cos\alpha z \end{cases} \quad at \quad r = R,$$

$$\frac{Q_{0}}{2\pi} = \psi(0,0) - \psi(R,0) \quad at \quad z = 0.$$
(3.20)

3.2.1 Non-dimensional Quantities

The following parameters are defined for non-dimensional analysis:

$$r' = \frac{r}{R}, \ z' = \frac{z}{R}, \ v_{r'} = \frac{v_r}{V_1}, \ v_{z'} = \frac{v_z}{V_1}, \ Q'_0 = \frac{Q_0}{V_1 R^2},$$

$$V'_0 = \frac{V_0}{V_1}, \ p' = \frac{p}{\mu V_1 R}, \ \Omega' = \frac{\Omega R}{V_1}, \ \psi' = \frac{\psi}{V_1 R^2}, \ \lambda^2 = \frac{R^2 \mu}{\xi}. \tag{3.21}$$

Eq. (3.22) takes the following form after using above non-dimensional quantities:

$$E^6\psi - \lambda^2 E^4\psi = 0, (3.22)$$

where

$$\lambda^2 = \frac{R^2 \mu}{\xi},\tag{3.23}$$

and dimensionless form of boundary conditions will take the following form:

$$\frac{\partial}{\partial r} \left(-\frac{1}{r} \frac{\partial \psi}{\partial r} \right) = 0, \quad \frac{1}{r} \frac{\partial \psi}{\partial z} = 0 \quad \text{at} \quad r = 0,$$

$$-\frac{1}{r} \frac{\partial \psi}{\partial r} = 0, \quad \frac{1}{r} E^2 \psi = 0, \quad \frac{1}{r} \frac{\partial \psi}{\partial z} = \begin{cases} V_0 \sin \alpha z \\ V_0 \cos \alpha z \end{cases} \quad \text{at} \quad r = 1,$$

$$\frac{Q_0}{2\pi} = \psi (0, 0) - \psi (R, 0) \quad \text{at} \quad z = 0,$$
(3.24)

3.3 Solution of the Problem

When the reabsorption of the tube wall is expressed as a sine function of the axial distance, the exact solution of Eq.(3.22) can be determined by defining the following stream function $\psi(r,z)$

$$\psi(r,z) = (\cos \alpha z) F(r) + G(r). \tag{3.25}$$

Similarly, when reabsorption of the wall follows a consine function of axial position, Eq.(3.22) can be solved exactly using the stream function $\psi(r, z)$.

$$\psi(r,z) = (\sin \alpha z) F(r) + G(r). \tag{3.26}$$

After using above function in Eq.(3.22) and (3.24), one can get the following systems of BVP's:

$$L_1^6 F(r) - \lambda^2 L_1^4 F(r) = 0, \tag{3.27}$$

where

$$L_1^2 = \left(\frac{d^2}{dr^2} - \frac{1}{r}\frac{d}{dr} - \alpha^2\right),\tag{3.28}$$

and associated boundary conditions are

$$F = 0,$$
 $\frac{d}{dr}\left(\frac{1}{r}\frac{dF}{dr}\right) = 0,$ at $r = 0,$ (3.29)

$$F = \frac{-V_0}{\alpha}, \quad \frac{1}{r}\frac{dF}{dr} = 0, \quad \left(\frac{d^2F}{dr^2} - \frac{1}{r}\frac{dF}{dr} - \alpha^2F\right) = 0, \quad \text{at} \quad r = 1,$$

The second BVP takes the following form:

$$E_1^6 G(r) - \lambda^2 E_1^4 G(r) = 0, \tag{3.30}$$

where

$$E_1^2 = \left(\frac{d^2}{dr^2} - \frac{1}{r}\frac{d}{dr}\right),\tag{3.31}$$

and boundary conditions for above system is given as follows:

$$G = 0,$$
 $\frac{d}{dr}\left(\frac{1}{r}\frac{dG}{dr}\right) = 0,$ at $r = 0,$ (3.32)

$$\frac{d}{dr}\left(\frac{1}{r}\frac{dG}{dr}\right)=0, \quad \ \frac{1}{r}\frac{dG}{dr}=0, \quad \text{ at } \quad r=1,$$

$$G(R) - G(0) = \frac{-Q_0}{2\pi} - (F(R) - F(0)), \text{ at } z = 0.$$

The solution of Eq.(3.27) can be represented as follows

$$\left(\frac{d^2}{dr^2} - \frac{1}{r}\frac{d}{dr} - \alpha^2\right)^2 \left(\frac{d^2}{dr^2} - \frac{1}{r}\frac{d}{dr} - (\alpha^2 + \lambda^2)\right) F(r) = 0,$$
(3.33)

Let

$$W_1 = \left(\frac{d^2}{dr^2} - \frac{1}{r}\frac{d}{dr} - \left(\alpha^2 + \lambda^2\right)\right)F(r). \tag{3.34}$$

The Eq.(3.33) become

$$\left(\frac{d^2}{dr^2} - \frac{1}{r}\frac{d}{dr} - \alpha^2\right)^2 W_1 = 0, \tag{3.35}$$

which is called modified bessel equation, The solution of Eq.(3.34) is

$$W_1 = r \left(c_1 I_1 \left(\alpha r \right) + c_2 K_1 \left(\alpha r \right) + r \left(c_3 I_2 \left(\alpha r \right) + c_4 K_2 \left(\alpha r \right) \right) \right). \tag{3.36}$$

where I_1 and I_2 represent modified Bessel function of first kind, K_1 and K_2 are modified bessel function of second kind. For bounded solution choose $c_2 = c_4 = 0$; leading to the following finite solution:

$$W_1 = r (c_1 I_1 (\alpha r) + r c_3 I_2 (\alpha r)). \tag{3.37}$$

The Eq.(3.35) become

$$\left(\frac{d^2}{dr^2} - \frac{1}{r}\frac{d}{dr} - \left(\alpha^2 + \lambda^2\right)\right)F(r) = r\left(c_1I_1\left(\alpha r\right) + rc_3I_2\left(\alpha r\right)\right). \tag{3.38}$$

The Eq.(3.38) is non-homogenous ordinary equation, the solution of Eq.(3.38) become

$$F(r) = rc_5 I_1 \left(r \sqrt{\alpha^2 + \lambda^2} \right) + rAI_1 \left(\alpha r \right) + \left(B + r^2 C \right) I_2 \left(\alpha r \right). \tag{3.39}$$

Using the remaining boundary conditions, we determine the values of A, B and c_5 which are listed in the appendix.

To find the solution of G(r), solve the following equation:

$$\left(\frac{d^2}{dr^2} - \frac{1}{r}\frac{d}{dr}\right)^2 \left(\frac{d^2}{dr^2} - \frac{1}{r}\frac{d}{dr} - \lambda^2\right) G(r) = 0,$$
(3.40)

where

$$\frac{d^2}{dr^2} - \frac{1}{r}\frac{d}{dr} = r\frac{d}{dr}\left(\frac{1}{r}\frac{d}{dr}\right). \tag{3.41}$$

Integrating both side of Eq.(3.40) one can get following form:

$$\left(\frac{d^2}{dr^2} - \frac{1}{r}\frac{d}{dr} - \lambda^2\right)G(r) = b_1\frac{r^4}{16} + b_2\frac{r^2}{2}\left(\ln r - \frac{1}{2}\right) + b_3\frac{r^2}{2} + b_4.$$
 (3.42)

To satisfy the boundary conditions at r = 0 we must have $b_2 = 0, b_3 = 0$; therefore, we obtain

$$\left(\frac{d^2}{dr^2} - \frac{1}{r}\frac{d}{dr} - \lambda^2\right)G(r) = b_1\frac{r^4}{16} + b_3\frac{r^2}{2}.$$
(3.43)

The solution of Eq.(3.43) become

$$G(r) = rb_5 I_1(\lambda r) - (D + Er^2) r^2.$$
 (3.44)

The values of C, D and b_5 are found using the remaining boundary conditions and are documented in the appendix.

Incorporating the solution of F(r) and G(r) into Eq.(3.25). The stream function for the case of sinusoidal reabsorption takes the following form.

$$\psi(r,z) = V_0(\cos\alpha z) \left(rc_5 I_1 \left(r\sqrt{\alpha^2 + \lambda^2} \right) + (rA) I_1(\alpha r) + \left(B + r^2 C \right) I_2(\alpha r) \right)$$

$$+ rb_5 I_1(\lambda r) - \left(D + Er^2 \right) r^2.$$

$$(3.45)$$

Using above stream function in Eq.(3.15), one can get the following velocity components:

$$v_r = \frac{-\alpha V_0 \sin(\alpha z) \left(rc_5 I_1 \left(r\sqrt{\alpha^2 + \lambda^2}\right) + (rA) I_1 (\alpha r) + \left(B + r^2 C\right) I_2 (\alpha r)\right)}{r}, \tag{3.46}$$

$$v_{z} = -\frac{V_{0}\cos(\alpha z)\left(r\alpha\left(2B - Ar^{2}\alpha\right)I_{0}\left(r\alpha\right) - c_{5}r^{3}\alpha\sqrt{\alpha^{2} + \lambda^{2}}I_{0}\left(r\sqrt{\alpha^{2} + \lambda^{2}}\right)\right) - \left(4B + r^{2}\left(B + Cr^{2}\right)\alpha^{2}\right)I_{1}\left(\alpha r\right)}{r^{3}\alpha} + 2D + 4Er^{2} - b_{5}\lambda I_{0}\left(\lambda r\right).$$

$$(3.47)$$

In a similar manner, substitute the solution F(r) and G(r) into Eq.(3.26). The stream function corresponding to the cosine function can be determined and is give as follows:

$$\psi(r,z) = V_0(\sin \alpha z) \left(rc_5 I_1 \left(r\sqrt{\alpha^2 + \lambda^2} \right) + (Ar + B) I_1(\alpha r) \right)$$

$$+ rb_5 I_1(\lambda r) - \left(D + Er^2 \right) r^2.$$
(3.48)

Substituting the above stream function into Eq.(3.15) yields the following velocity components.

$$v_r = \frac{V_0 \alpha \cos(\alpha z) \left(r c_5 I_1 \left(r \sqrt{\alpha^2 + \lambda^2} \right) + + (rA) I_1 (\alpha r) + \left(B + r^2 C \right) I_2 (\alpha r) \right)}{r}, \quad (3.49)$$

$$v_{z} = -\frac{V_{0} \sin (\alpha z) \left(r\alpha \left(2B - Ar^{2}\alpha\right) I_{0} \left(r\alpha\right) - c_{5}r^{3}\alpha\sqrt{\alpha^{2} + \lambda^{2}} I_{0} \left(r\sqrt{\alpha^{2} + \lambda^{2}}\right) - \left(4B + r^{2} \left(B + Cr^{2}\right)\alpha^{2}\right) I_{1} \left(\alpha r\right) \right)}{r^{3}\alpha} + 2D + 4Er^{2} - b_{5}\lambda I_{0} \left(\lambda r\right).$$

$$(3.50)$$

With the help of Eq. (3.6) - (3.7), one can get the expression for pressure distribution and similarly, by substituting the values for the derived velocity components in Eq. (3.9), we can find out the value for shear stress at the wall of the tube.

3.4 Result and Discussion

To observe how emerging parameters effect the fluid flow, we have presented the graphical results in this section. The influence of periodic reabsorption velocity $V_0 \sin(\alpha z)$ and couple stress parameter λ is represented by radial and axial velocity, pressure distribution and shear stress at the wall.

3.4.1 Effect of Reabsorption Parameter V_0 :

The variation in radial velocity for different values of re-absorption parameter V_0 is depicted in Fig. 3.2 (a). At the axis of the tube, the radial flow remains stationary, while flow rises due to re-absorption near the boundary. It is also noticed that rising effect is more pronounced for cosine type of the re-absorption as compared with sine re-absorption. Fig. 3.2(b) demonstrates the influence of re-absorption rate V_0 on axial velocity it shows that flow in axial direction rises when the re-absorption rate surges near the synovial membrane. The flow along the axial direction of tube is significantly stronger when re-absorption rate of the nutrients is cosine type. Fig. 3.2(c) illustrates that load in the synovial fluid is effected by re-absorption rate of the nutrients and indicating that pressure produced in synovial fluid surges as the re-absorption rate of nutrients become high in the synovial joint. It is also noticed that internal pressure in synovial fluid is more prominent when the nutrients have cosine type of re-absorption rate whereas the change in pressure gradient becomes steeper compared to sine type of re-absorption rate. Fig. 3.2(d) highlights the impact of re-absorption rate V_0 of nutrients on wall shear stress and causes to increase the shearing force near the synovium due to re-absorption rates of nutrients. This simulation indicates if nutrient re-absorption rate has cosine type of reabsorption, then the shearing forces become dominant as compare with sine type of re-absorption rate.

3.4.2 Effect of Couple-Stress Parameter λ :

The impact of the couple-stress parameter λ on radial and axial velocity is illustrated in Fig. 3.3(a-b) for both cosine and sine type re-absorption rate of nutrients. In both scenarios flow along the radial and axial direction retarded due to surge in couple stress viscosity parameter λ the surge in viscosity causes to increase in resistive forces that opposes fluid motion along and across the tube. The increase in frictional forces make the trouble for the synovial fluid flow therefore the moderate viscosity of couple stress is good for the lubrication of joint. Also, decay in axial flow is more pronounced for cosine re-absorption rate of nutrients as compared to sine re-absorption rate. Fig. 3.3(c) shows that rise in fluid viscosity leads to more load for the lubrication of joint for both sine and cosine re-absorption rate. The high resistance in fluid flow makes the flow thick that requires the more pressure to lubricate the joint for both cosine and sine re-absorption rate. The pressure is more dominant for cosine re-absorption as

compared with sine re-absorption. Lastly, Fig. 3.3(d) display the variation in wall shear stress against the couple stress fluid parameter λ , it shows that the fluid requires more stress along the synovium when the micro-rotation decreases and its ratio with viscosity increases. This behavior is attributed due to the influence of viscous forces in synovial fluid. It is also noticed that when the re-absorption rate of the nutrients is cosine the shearing forces are larger as compared with the sine re-absorption rate of nutrients.

3.4.3 Effect of Periodicity Parameter α :

The impact of the periodicity parameter α on radial and axial velocity is illustrated in Fig. 3.4(a-b) for both sine and cosine type of re-absorption rate. In both scenarios flow along the radial and axial direction retarded due to surge in periodicity parameter for the case of cosine but the radial and axial flow in case of sine type of re-absorption. Also, decay in axial and radial flow is more pronounced for cosine type of re-absorption rate of nutrients as compared to sine type of re-absorption rate. Fig. 3.4(c) shows that rise in periodicity leads to more load for the lubrication of joint for both cosine and sine type of re-absorption rate. The high resistance in the fluid flow makes the flow thick that requires the more pressure to lubricate the joint for both sine and cosine type of re-absorption rate. The pressure is more dominant for cosine type of re-absorption as compared with sine type of re-absorption. Lastly, Fig. 3.4 (d) display the variation in wall shear stress against the periodicity parameter α it shows that the fluid requires more stress along the synovium when the periodicity decreases. It is also noticed that when the re-absorption rate of the nutrients is cosine the shearing forces are larger as compared with the sine type of re-absorption rate of nutrients.

3.4.4 Effect of Initial Flow Rate Q_0

The impact of the flow rate Q_0 on axial velocity is illustrated in Fig. 3.5(a) for both sine and cosine re-absorption rate of nutrients. In case of cosine reabsorption the flow along the axial direction retarded but for the case of sine reabsorption the flow rate causes to rise in axial flow. Fig.3.5(b) shows that rise in flow are leads to less load for the lubrication of joint for both sine and cosine re-absorption rate. The pressure is more dominant for cosine type of re-absorption as compared with sine re-absorption. Lastly, Fig. 3.5(c) display the variation in wall shear

stress against the flow rate Q_0 , it shows that the fluid requires more stress along the synovium for the case of sine reabsorption but less for the case of cosine reabsorption.

3.4.5 Effect of Axial Position on velocities:

The impact of the axial position on radial and axial velocity is illustrated in Fig. 3.6(a-b) for both cosine and sine type of re-absorption rate of nutrients. In both scenarios flow along the radial and axial direction retarded due to surge in axial position.

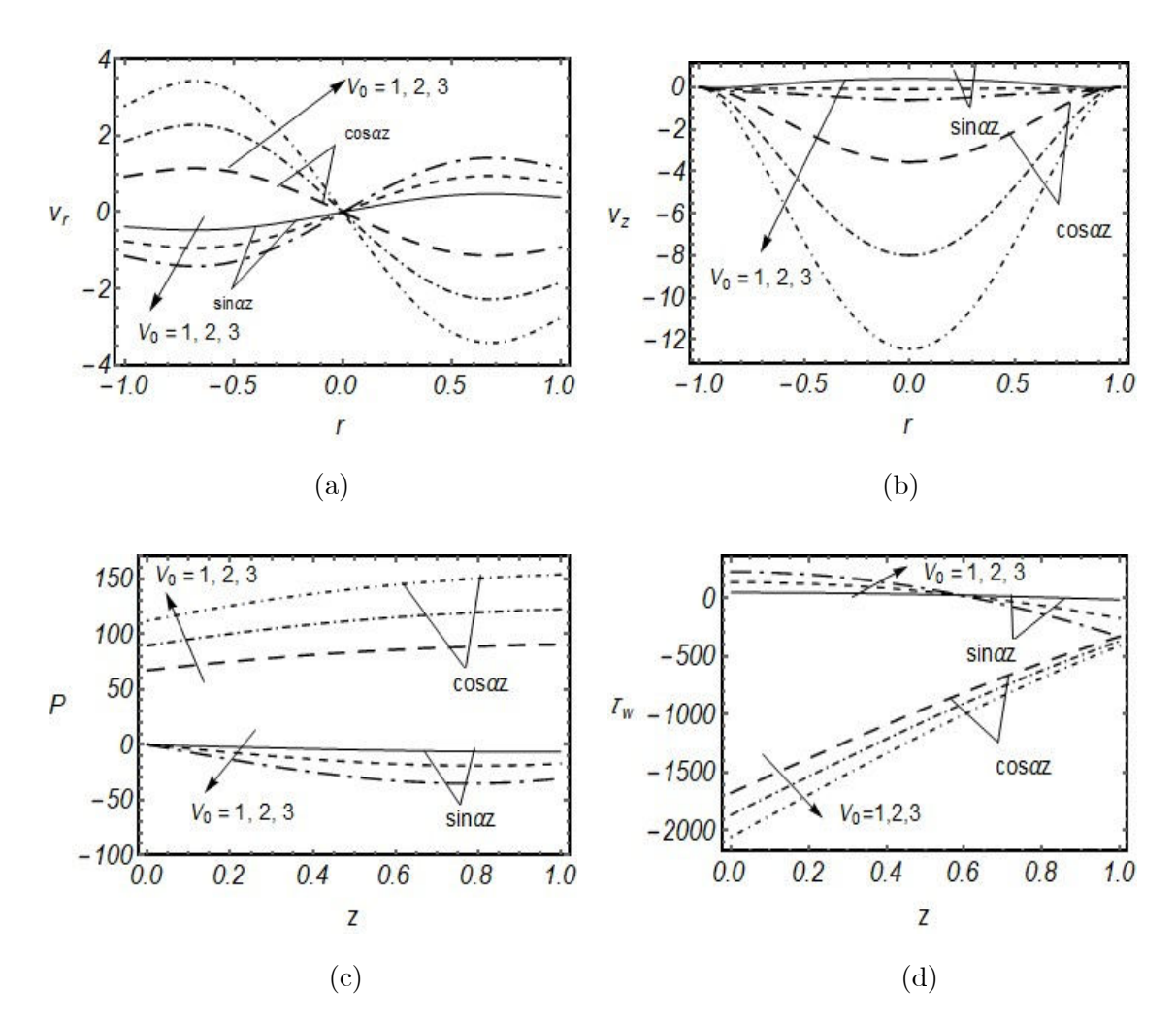


Fig. 3.2a (a-d): Influence of reabsorption parameter V_0 on (a) radial velocity, (b) axail velocity, (c) pressure distribution, and (d) wall shear stress.

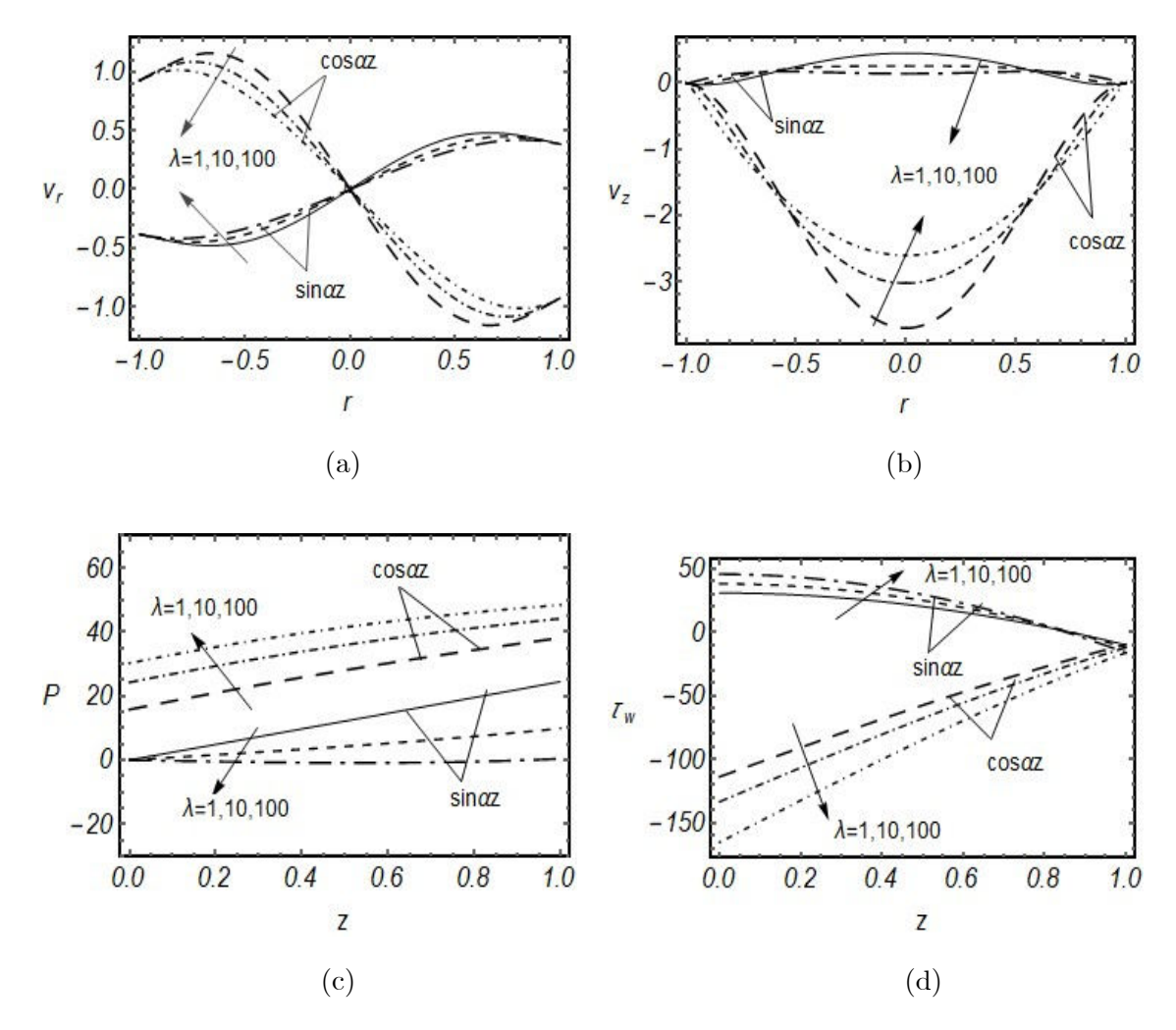
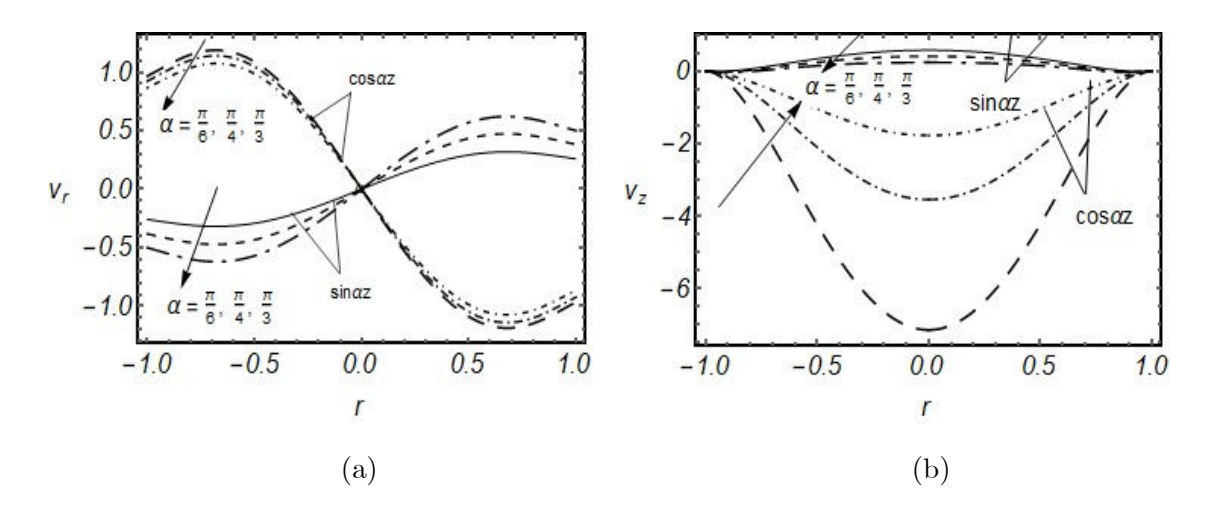


Fig. 3.3a (a-d): Influence of couple stress parameter λ on (a) radial velocity , (b) axail velocity, (c) pressure distribution, and (d) wall shear stress.



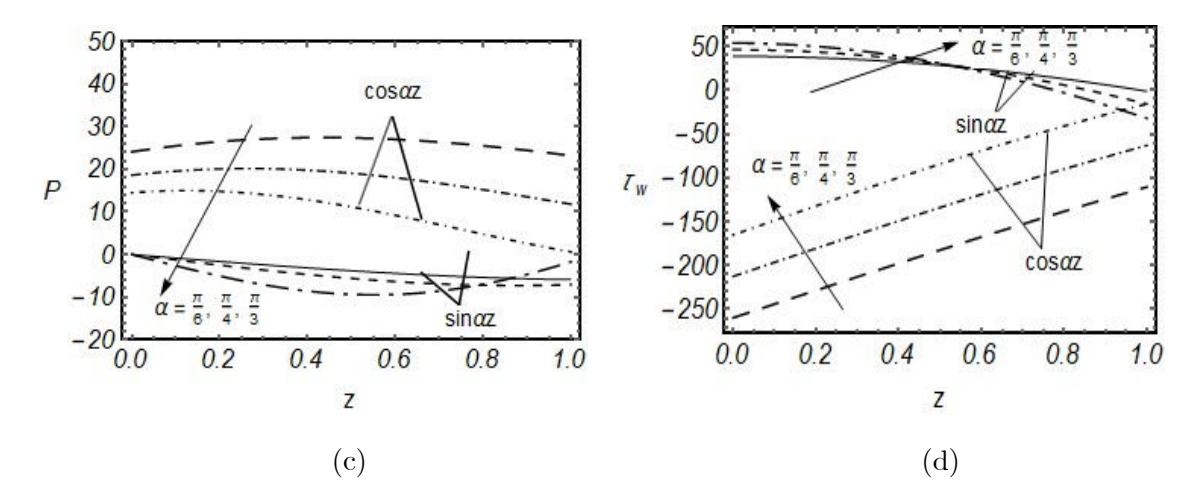


Fig. 3.4a (a-d): Influence of periodic reabsorption parameter α on (a) radial velocity, (b) axail velocity, (c) pressure distribution, and (d) wall shear stress.

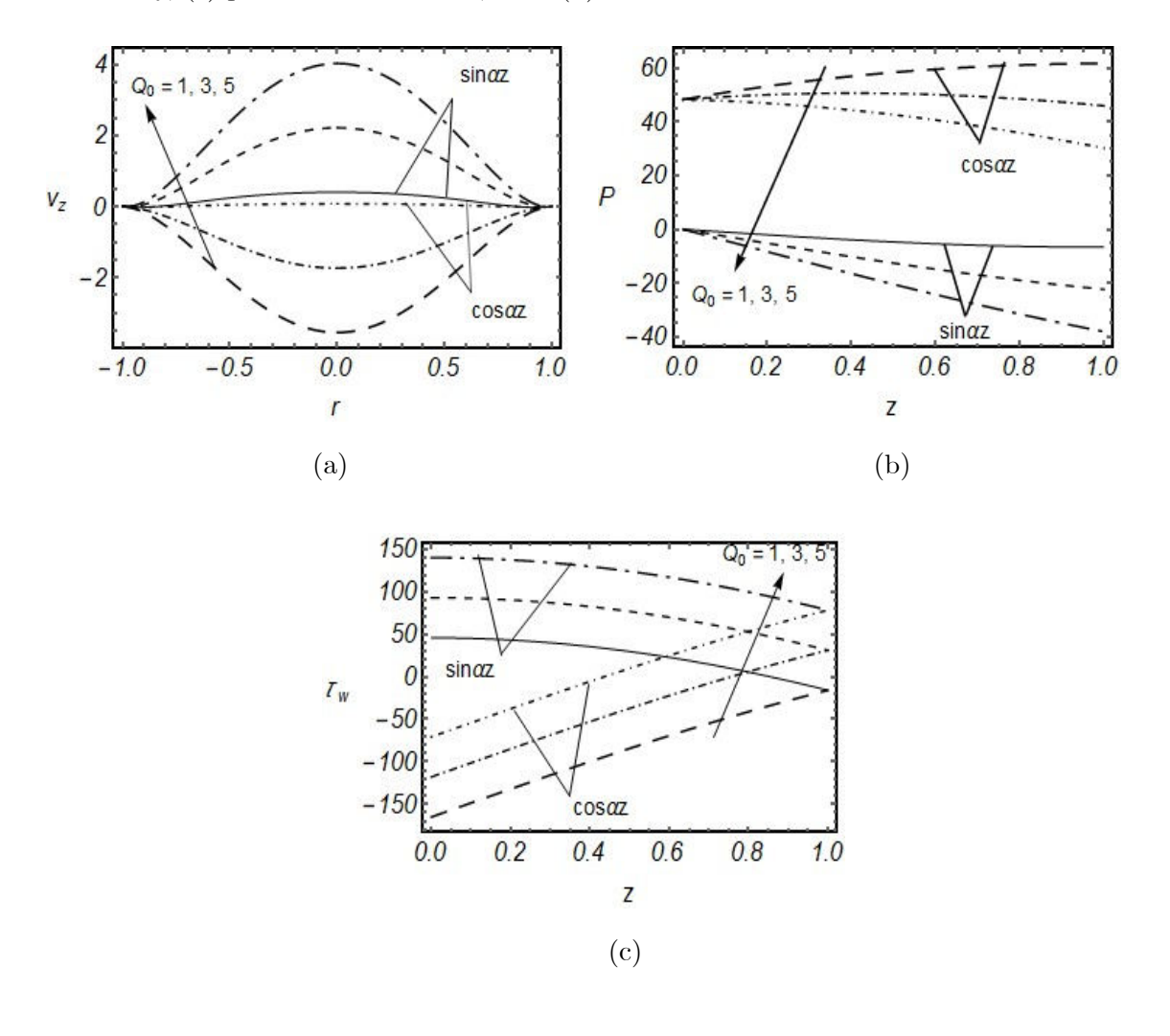


Fig. 3.5a(a-c): Influence of Volumetric flow rate Q_0 on (a) axial velocity, (b) pressure distribution, and (c) wall shear stress.

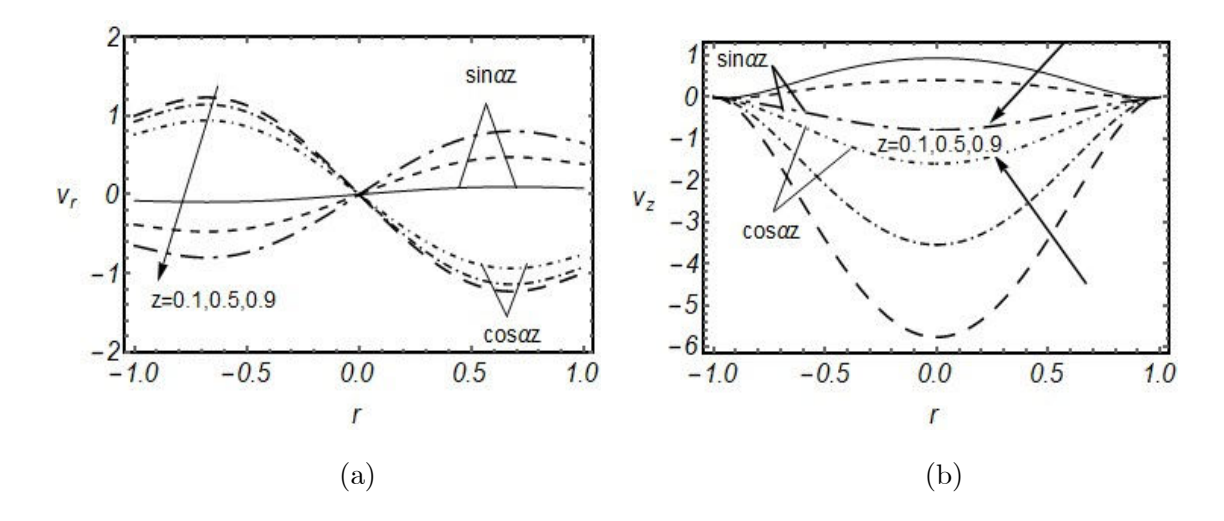


Fig. 3.6a (a-b): Variation in axial and radial at entry, middle and exit region of the tube.

3.5 Conclusion

In this research a mathematical model is described by a finite-length permeable tube filled with couple-stress fluid (synovial fluid) and rheological properties of the fluid are observed by the laws of fluid mechanics which are simulated by the software Mathematica. The outcomes of the study reveal that flow along the tube become fast when the nutrients from the synovial fluid reabsorb at cosine type of rate as compared with sine type of rate whereas the flow across the tube become fast when the re-absorption rate of nutrients is cosine as compared with sine rate. Load and shear stress within the synovial fluid become high when the nutrients in synovial fluid reabsorb with cosine rate as compared with sine rate. The radial and axial velocity components, pressure variation, and shear stress show similar trends in both Newtonian and couple stress fluids. However, the couple stress fluid shows greater amplitude in all these quantities due to the presence of microstructural effects. This indicates that the couple stress parameter enhances the magnitude of velocity, pressure, and stress without changing the overall pattern of their distribution.

3.6 Appendix

$$A = \frac{-4c_1}{\left(\alpha^2 + 4\lambda^2\right)} + \frac{12\alpha c_3}{\left(\alpha^2 + 4\lambda^2\right)\left(\alpha^2 + \lambda^2\right)},$$

$$B = \left(\frac{-8c_1}{\alpha\left(\alpha^2 + 4\lambda^2\right)} + \frac{24c_3}{\left(\alpha^2 + 4\lambda^2\right)\left(\alpha^2 + \lambda^2\right)}\right),$$

$$C = \frac{-2c_3}{\alpha^2 + \lambda^2},$$

$$D = \left(\frac{\lambda^2 b_3 + b_1}{2\lambda^4}\right)r^2,$$

$$E = \frac{b_1 r^4}{16\lambda^2}.$$

Bibliography

- Yin, W., & Frame, M. D. (2011). Biofluid Mechanics: An Introduction to Fluid Mechanics, Macrocirculation, and Microcirculation. Academic Press.
- [2] Lai, W. M., Kuei, S. C., & Mow, V. C. (1978). Rheological equations for synovial fluids. Journal of Biomechanical Engineering, 100(4), 169–186.
- [3] Ouerfelli, N., Vrinceanu, N., Mliki, E., Amin, K. A., Snoussi, L., Coman, D., & Mrabet, D. (2024). Rheological behavior of the synovial fluid: a mathematical challenge. Frontiers in Materials, 11, 1386694.
- [4] Singh, K. I., Sobti, V. K., & Srivastava, A. K. (1999). Clinical, radiological, hematological and synovial fluid observations on the effect of an antiarthritic drug (ART) in experimental aseptic acute arthritis in equines. Journal of Equine Veterinary Science, 19(8), 511-517.
- [5] Hasnain, S., Abbas, I., Al-Atawi, N. O., Saqib, M., Afzaal, M. F., & Mashat, D. S. (2023). Knee synovial fluid flow and heat transfer, a power law model. Scientific Reports, 13(1), 18184.
- [6] Maqbool, K., Siddiqui, A. M., Mehboob, H., & Tahir, A. (2024). Dynamics of non-Newtonian synovial fluid through permeable membrane with periodic filtration. International Journal of Modern Physics B, 38(19), 2450251.
- [7] Maqbool, K., Siddiqui, A. M., Mehboob, H., & Jamil, Q. (2022). Study of non-Newtonian synovial fluid flow by a recursive approach. Physics of Fluids, 34(11).
- [8] Ramanaiah, G. (1979). Squeeze films between finite plates lubricated by fluids with couple stress. Wear, 54(2), 315-320.

- [9] Ramanaiah, G., & Sarkar, P. (1979). Slider bearings lubricated by fluids with couple stress. Wear, 52(1), 27-36.
- [10] Sinha, P., & Singh, C. (1981). Couple stresses in the lubrication of rolling contact bearings considering cavitation. Wear, 67(1), 85-98.
- [11] Hayat, T., Sajjad, R., Alsaedi, A., Muhammad, T., & Ellahi, R. (2017). On squeezed flow of couple stress nanofluid between two parallel plates. Results in physics, 7, 553-561.
- [12] Bashir, S., & Sajid, M. (2022). Flow of two immiscible uniformly rotating couple stress fluid layers. Physics of Fluids, 34(6).
- [13] Madasu, K. P., & Sarkar, P. (2022). Couple stress fluid past a sphere embedded in a porous medium. Archive of Mechanical Engineering, 5-19. OR (Raptis, A. (1982). Effects of couple stresses on the flow through a porous medium. Rheologica Acta, 21, 736-737).
- [14] Ahmed, S., Bég, O. A., & Ghosh, S. K. (2014). A couple stress fluid modeling on free convection oscillatory hydromagnetic flow in an inclined rotating channel. Ain Shams Engineering Journal, 5(4), 1249-1265.
- [15] Srivastava, L. M. (1985). Flow of couple stress fluid through stenotic blood vessels. Journal of Biomechanics, 18(7), 479-485. OR (Sahu, M. K., Sharma, S. K., & Agrawal, A. K. (2010). Study of arterial blood flow in stenosed vessel using non-Newtonian couple stress fluid model. International Journal of Dynamics of Fluids, 6(2), 209-219).
- [16] Pozrikidis, C. (2010). Stokes flow through a permeable tube. Archive of Applied Mechanics, 80, 323-333.
- [17] Shankar, V. (2015). Stability of fluid flow through deformable tubes and channels: an overview. Sadhana, 40(3), 925-943.
- [18] Siddiqui, A. M., Sohail, A., & Maqbool, K. (2017). Analysis of a channel and tube flow induced by cilia. Applied Mathematics and Computation, 309, 133-141.
- [19] Siddiqui, A. M., Sohail, A., Naqvi, S., & Haroon, T. (2017). Analysis of Stokes flow through periodic permeable tubules. Alexandria Engineering Journal, 56(1), 105-113.

- [20] Maiti, S., & Pandey, S. K. (2017). Rheological fluid motion in tube by metachronal waves of cilia. Applied Mathematics and Mechanics, 38, 393-410.
- [21] Jeong, J. T. (2018). Axisymmetric Stokes flow due to the motion of a thin disk along the axis of a circular tube. European Journal of Mechanics-B/Fluids, 67, 397-403.
- [22] Farooq, M. U., Rehman, A., & Sheikh, N. (2023). Annular Axisymmetric Stagnation Flow of a Casson Fluid Through Porous Media in a Moving Cylinder. American Journal of Modern Physics, 12(3), 47-53.
- [23] Hakligor, I. M., Ozkan, G. M., & Akilli, H. (2025). Flow structures in the near wake of permeable circular cylinders in shallow water. European Journal of Mechanics-B/Fluids, 111, 295-307.